Environmental Science & Technology

Article

pubs.acs.org/est

Sulfurization of Dissolved Organic Matter Increases Hg–Sulfide–Dissolved Organic Matter Bioavailability to a Hg-Methylating Bacterium

Andrew M. Graham,*[,†] Keaton T. Cameron-Burr,[†] Hayley A. Hajic,[†] Connie Lee,[†] Deborah Msekela,[†] and Cynthia C. Gilmour[‡]

[†]Department of Chemistry, Grinnell College, 1116 Eighth Avenue, Grinnell, Iowa 50112, United States

[‡]Smithsonian Environmental Research Center, 647 Contees Wharf Road, Edgewater, Maryland 21037, United States

Supporting Information

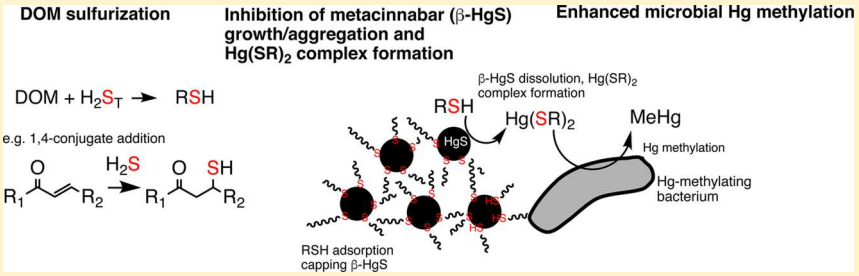

ABSTRACT: Reactions of dissolved organic matter (DOM) with aqueous sulfide (termed sulfurization) in anoxic environments can substantially increase DOM's reduced sulfur functional group content. Sulfurization may affect DOM–trace metal interactions, including complexation and metal-containing particle precipitation, aggregation, and dissolution. Using a diverse suite of DOM samples, we found that susceptibility to additional sulfur incorporation via reaction with aqueous sulfide increased with increasing DOM aromatic-, carbonyl-, and carboxyl-C content. The role of DOM sulfurization in enhancing Hg bioavailability for microbial methylation was evaluated under conditions typical of Hg methylation environments (μM sulfide concentrations and low Hg-to-DOM molar ratios). Under the conditions of predicted metacinnabar supersaturation, microbial Hg methylation increased with increasing DOM sulfurization, likely reflecting either effective inhibition of metacinnabar growth and aggregation or the formation of Hg(II)–DOM thiol complexes with high bioavailability. Remarkably, Hg methylation efficiencies with the most sulfurized DOM samples were similar (>85% of total Hg methylated) to that observed in the presence of L-cysteine, a ligand facilitating rapid Hg(II) biouptake and methylation. This suggests that complexes of Hg(II) with DOM thiols have similar bioavailability to Hg(II) complexes with low-molecular-weight thiols. Overall, our results are a demonstration of the importance of DOM sulfurization to trace metal and metalloid (especially mercury) fate in the environment. DOM sulfurization likely represents another link between anthropogenic sulfate enrichment and MeHg production in the environment.

1. INTRODUCTION

Dissolved organic matter (DOM) plays a key role in the mobility and bioavailability of mercury (Hg) in aquatic systems. At the ecosystem scale, the flux of mercury in coastal[1] and terrestrial[2] ecosystems is tightly coupled to dissolved organic carbon (DOC) flux, as inorganic Hg(II) ($Hg(II)_i$) forms strong complexes with thiol moieties in DOM.[3] Within the anoxic, often sulfidic, environments, where Hg methylation occurs, such as bottom sediments, wetlands, and flooded soils, the importance of DOM is likely in slowing the growth and aggregation of β-HgS (metacinnabar) particles.[4−7] Inhibition of β-HgS growth and aggregation is hypothesized to support the increased rates of microbial Hg methylation,[8−10] as smaller Hg–S clusters and particles are more bioavailable to Hg-methylating bacteria,[10] a process that remains incompletely understood. Additionally, dissolved Hg–DOM complexes may be bioavailable for microbial Hg uptake and subsequent methylation.[11,12]

Hg methylation by a model Hg-methylating bacterium suspended in Hg–sulfide–DOM solutions correlated with both DOM aromaticity and sulfur content.[9] This suggested the importance of both nonspecific (increased inhibition of β-HgS precipitation and aggregation by more-aromatic and more-surface-active DOM) and specific (capping of β-HgS by DOM thiols or formation of Hg–DOM thiol complexes) interactions between DOM and Hg in controlling Hg bioavailability under sulfidic conditions. In this paper, we further explore the relationship between DOM composition and Hg bioavailability

Received: May 30, 2017
Revised: July 7, 2017
Accepted: July 13, 2017
Published: July 13, 2017

DOI: 10.1021/acs.est.7b02781
Environ. Sci. Technol. XXXX, XXX, XXX–XXX

for methylation. Specifically, we focus on how diagenetic sulfurization of DOM (the incorporation of sulfur into DOM) influences the Hg−sulfide−DOM interactions that determine, in part, the rate and extent of Hg methylation in anoxic environments.

In a broader context, most studies on the role of DOM in trace metal complexation and metal-containing particle growth and aggregation have focused on DOM isolated from oxic surface waters. There is growing recognition that DOM isolated from oxic surface waters may not be representative of that found in highly stratified lakes, sediment porewaters, and groundwaters in which sulfate reduction is an important biogeochemical process. Sulfide produced from microbial sulfate reduction can be readily incorporated into DOM via S_N2, S_NAr, and Michael addition reactions, as demonstrated in a number of studies in which sulfide was reacted with model compounds[13,14] as well as extracted natural DOM samples.[15−17] High-resolution mass spectrometric studies of DOM composition in the North American prairie pothole region[18] and the Florida Everglades[19,20] indicate that CHOS and CHONS compounds can reach 10 to nearly 50% of all identified molecular formulas. Sulfurization is relatively rapid, occurring on a time scale of days for environmentally relevant concentrations of DOM and sulfide.[17] The products of sulfurization identified by X-ray absorption near-edge spectroscopy (XANES) include both reduced (thiol and disulfide species) as well as oxidized (e.g., sulfoxides, sulfones, sulfonates, and sulfate esters) species, although there is evidence that the proportion of reduced S species increases with increasing degree of sulfurization.[16,20]

Here, we describe experiments in which the sulfur content of a suite of DOM samples was directly manipulated by reacting DOM samples with hydrogen sulfide and bisulfide at room temperature. We subsequently evaluated microbial Hg methylation in solutions containing mg/L concentrations of our suite of the sulfurized DOM samples and μM concentrations of sulfide, mimicking conditions found in many anoxic environments. Our experiments provide information on the role of DOM sulfurization in controlling Hg bioavailability to Hg-methylating bacteria and shed additional light on the mechanisms of $Hg(II)_i$ uptake and methylation in sulfidic environments.

2. EXPERIMENTAL SECTION

2.1. Dissolved Organic Matter Samples. Dissolved organic matter samples with a range of average molecular weight, aromaticity, and native sulfur content were purchased from the International Humic Substances Society (IHSS) for use in the DOM sulfurization experiments. The four samples included humic and fulvic acids from a blackwater river draining the Okeefenokee Swamp in Georgia (Suwanee River humic and fulvic acids; SRHA standard II and SRFA standard II), a fulvic acid from a high latitude (60 °N) drinking water reservoir in Norway (Nordic Lake fulvic acid; NLFA); and a microbially derived fulvic acid from a eutrophic Antarctic pond (Pony Lake fulvic acid; PLFA). The PLFA sample is unique among our samples in its high native sulfur content (3.03% by mass compared to 0.4−0.6% for the other DOM samples). Sulfur speciation determined by XANES was available for three of the four DOM samples (SRHA, SRFA, and PLFA); reduced exocyclic and heterocyclic sulfur comprised 53−68% of total sulfur for these samples and is likely similar for NLFA based on analysis of Nordic Lake humic acid (71.8% of total S as reduced S).[21] Characteristics of the DOM samples are summarized in Table 1.

2.2. DOM Sulfurization Reactions. Inside an anoxic glovebag (Coy Laboratory Products) with an atmosphere of 2−5% H_2 and 95−98% N_2, maintained O_2-free with Pd catalysts, DOM samples were dissolved to ∼500 mg C/L in N_2-degassed deionized water (DDIW). The stock solution was aliquoted into foil-wrapped borosilicate glass serum bottles, and solutions were spiked with Na_2S to give total sulfide (H_2S_T) additions of 0 to 50 mmol S/mol C, with four to five different S-to-C ratios evaluated for each DOM sample. The pH of each solution was adjusted to the pH of the unspiked DOM solution (∼5.0) with degassed trace metal grade HNO_3. The serum bottles (containing a liquid-to-headspace ratio of >10:1) were then immediately stoppered and allowed to react for 48 h at room temperature. The pH and range of S/C additions were similar to that employed in a study of As sorption to sulfurized OM.[16] Notably, Hoffmann et al.[16] found minimal impact of pH on DOM sulfurization in the pH range of 5.0−7.0. The incubation time (48 h) was selected to yield maximal S incorporation based on kinetic investigations of S incorporation into DOM.[16,17]

Following the 48 h reaction period, sulfurized DOM was recovered by solid-phase extraction (SPE)[22] carried out in the anoxic glovebag. Sulfurized DOM samples were acidified to pH 2.0 with degassed 50% v/v trace metal-grade HCl and then passed through conditioned 3 mL Agilent Bond Elut PPL columns (100 mg of styrene−divinylbenzene polymer; pore size of 150 Å) at a flow rate of ∼2 mL/min. Salts (including unreacted Na_2S) were removed by washing with two column volumes of 0.01 M degassed HCl. The columns were then dried by drawing an anoxic atmosphere through the columns at constant vacuum. Sulfurized DOM was eluted with 10 mL of high-performance liquid chromatography grade methanol (Fisher). Methanolic DOM solutions were evaporated under a gentle N_2 stream and then reconstituted in DDIW inside the glovebag. Similar to previous reports,[22] DOM recovery ranged from 32 to 81% of total DOC among all DOM samples (mean: 53 ± 18%), with lower variability (3−17% RSD) for each subtreatment of a single DOM sample (recoveries for individual samples reported in Table SI-1). Analysis of UV−vis spectra for sulfurized samples indicated that our sulfurization and SPE procedure did not substantially alter the size or aromaticity of a given DOM isolate. For example, for a given isolate, no correlations were observed between sulfur incorporation and the slope ratio[23] of the DOM sample recovered by SPE (reported in Table SI-1). Sulfurized DOM samples were stored in airtight stoppered bottles at 4 °C for no more than 5 days prior to initiation of Hg bioavailability assays. For each set of DOM samples, we included an unsulfurized DOM control subjected to the identical SPE recovery procedure as the sulfurized samples. SPE recovery and optical properties of the unsulfurized DOM samples were quite similar to that of sulfurized samples.

2.3. Hg Methylation Assays. Hg bioavailability for microbial methylation was determined in washed-cell assays in polypropylene tubes with the model organism *Desulfovibrio desulfuricans* ND132, an efficient Hg methylator[24,25] previously used to study Hg methylation in solutions containing DOM and sulfide.[8,9] Strain ND132 was grown to mid-log phase on an estuarine pyruvate−fumarate (EPF) medium[24] at 31 °C, centrifuged at 3000*g* for 15 min to pelletize cells, then resuspended in a minimal pyruvate−fumarate media (compo-

DOI: 10.1021/acs.est.7b02781
Environ. Sci. Technol. XXXX, XXX, XXX−XXX

Table 1. Select Characteristics of Dissolved Organic Matter Isolates Utilized in This Study[a]

isolate	description	sulfur content and speciation					carbon distribution by ^{13}C NMR[b]			
		native S content (weight %)[b]	native S-to-C ratio (mmol S/mol C) of raw DOM[b]	measured S-to-C ratio of unsulfurized SPE DOM (mmol S/mol C)[c]	percent S exocyclic[d]	percent S heterocyclic[d]	percent aromatic	percent carbonyl	percent carboxyl	percent acetal and (hetero) aliphatic
Suwannee River humic acid (SRHA, standard II)	Blackwater river draining Okeefenokee Swamp, sampled at Fargo, GA	0.54	4.14	3.42 ± 0.42	23.6	40.4	31	6	15	49
Suwannee River fulvic acid (SRFA, standard II)	Blackwater river draining Okeefenokee Swamp, sampled at Fargo, GA	0.46	3.15	1.88 ± 0.23	25.8	27.6	22	5	17	57
Nordic Lake fulvic acid	drinking water reservoir in Vallsjøen, Skarnes, Norway	0.58	3.30	3.12 ± 0.39	nd	nd	31	10	24	37
Pony Lake fulvic acid	shallow eutrophic saline pond in Anarctica	3.03	21.7	11.0 ± 1.4	46.9	21.3	12	1.2	17	69.6

[a]Superscripts indicate reference for characterization data. [b]Data are from the International Humic Substances Society. Note that percentages for carbon distribution do not necessarily add up to 100. Other elemental composition data for these samples also available at http://www.humicsubstances.org/elements.html. [c]This study. Measured S-to-C ratio on native (unsulfurized) DOM sample after recovery by solid-phase extraction (SPE). [d]Data are from Manceau and Nagy,[21] determined by XANES spectroscopy. [e]nd: no data available.

sition in Graham et al.).[8] Cells were centrifuged a second time, and methylation assays were initiated by resuspending cells in filter-sterilized minimal media that had been amended with 0.41 nM enriched inorganic $^{201}Hg(II)_i$ (in 1% v/v HCl) and ~10 mg C/L of sulfurized DOM, reduced with 25 μM titanium nitrilotriacetic acid (TiNTA) to remove trace oxygen contamination, and pre-equilibrated for 24 h at 31 °C. The 24 h pre-equilibration period was selected based on kinetic investigations of Hg−DOM complexation.[26] No external additions of sulfide were necessary, as strain ND132 cleaves the S−C bond in cysteine provided in growth medium releasing low (and reproducible) μM sulfide concentrations (range of 0.1 to 5.9 μM) in the cysteine-free (excepting positive controls described below) minimal assay medium. As noted below, a portion of the $^{201}Hg(II)_i$ spike was lost to bottle-wall adsorption during the ^{201}Hg and DOM pre-equilibration period, and observed total ^{201}Hg concentrations were typically between 0.1 to 0.3 nM. Cell suspensions were sampled immediately for the measurement of pH, optical density at 660 nm (OD_{660}), and sulfide (H_2S_T), and then placed in a 31 °C incubator inside the glovebag for 3 h. At the end of the incubation period, cell suspensions were sampled for total Hg (THg), total MeHg, filter-passing (0.2 μm nylon membrane) THg, pH, OD_{660}, and H_2S_T. Experimental timeframes (3 h) were selected on the basis of previous kinetic experiments demonstrating a plateau in MeHg production by strain ND132 within this time frame.[25] Control experiments included DOM-free controls, positive controls with 500 μM L-cysteine, conditions that favor high rates of MeHg production,[25,27] and unsulfurized-DOM controls. Our previous work demonstrated that Hg methylation was insignificant (<0.2% of ^{201}Hg spike methylated) in abiotic controls including DOM,[8] and these controls were not repeated for this investigation. All experiments, including controls, were performed in triplicate except for experiments with the NLFA isolate, which were performed in duplicate.

2.4. Analytical Methods. Total S content in sulfurized DOM samples was determined by inductively coupled plasma mass spectrometry (ICP-MS; Agilent 7500 CE), with monitoring of S at $m/z = 34^+$ and calibration against Na_2SO_4 standards following blank correction. While an isobaric interference at $m/z = 34^+$ due to $^{16}O^{18}O$ limits trace S determination by inductively couple plasma mass spectrometry (ICP-MS) collision or reaction cell technology, S concentrations in our DOM samples could readily be determined by monitoring at $m/z = 34^+$ following blank correction, as sample concentrations (60−470 μM) were substantially above the method detection limit (19.6 μM, determined based on three times the blank standard deviation). Relative percent difference (RPD) for duplicate analysis of S concentration averaged 12.4 ± 14.3% (n = 4 pairs). Dissolved organic carbon (DOC) concentrations of DOM samples recovered by SPE (along with initial stocks prior to sulfurization and SPE) were determined as nonpurgeable organic carbon using a Shimadzu TOC-V analyzer. Experimentally determined S-to-C ratios for DOM samples were calculated based on measured S and DOC concentrations.

Unfiltered cell suspensions were analyzed for THg by first digesting 1 mL of sample with 5 mL of 7:4 HNO_3/H_2SO_4 at ~190 °C and then amending with 1% v/v BrCl. Filtered samples were digested overnight in 1% BrCl at room temperature. THg analysis was carried out using online reduction with $SnCl_2$ and introduction of elemental Hg vapor directly into the ICP-MS.[8] MeHg concentrations were

DOI: 10.1021/acs.est.7b02781
Environ. Sci. Technol. XXXX, XXX, XXX−XXX

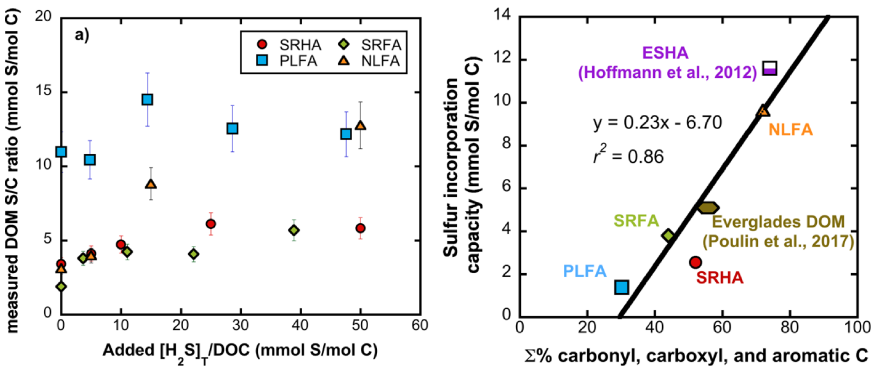

Figure 1. (a) Extent of total sulfur incorporation into dissolved organic matter as a function of the added sulfide-to-DOC ratio. (b) Relationship between bulk DOM functional group content determined by ^{13}C NMR and the total sulfur incorporation capacity. Sulfur incorporation capacity defined as the maximum change in DOM S content upon reaction with sulfide. For the NLFA sample and the Everglades DOM,[20] a plateau in DOM S content was not observed, so the reported S incorporation capacity should be interpreted as a minimum value. PLFA, Pony Lake fulvic acid; SRHA, Suwannee River humic acid; SRFA, Suwannee River fulvic acid; NLFA, Nordic lake fulvic acid; ESHA, Elliott soil humic acid. Data for ESHA came from Hoffmann et al.[16] Data for the Everglades DOM came from Poulin et al.,[20] with functional group content estimated based on data in Waples et al.[33]

determined by steam-distillation, aqueous-phase ethylation with sodium tetraethylborate, and gas chromatography (GC)−ICP-MS using isotopically enriched $Me^{199}Hg$ as an internal standard.[28] Herein, we report concentrations of excess ^{201}THg and $Me^{201}Hg$ after correction for contributions of (1) ambient THg or MeHg and (2) internal standard $Me^{199}Hg$. We routinely analyzed duplicate samples, standard reference materials (SRMs), and blanks as part of our quality assurance and quality control (QA/QC) efforts; a summary of QA/QC data is presented in Table SI-2.

Sulfide was analyzed using a silver and sulfide ion specific electrode with a Ag−AgCl reference electrode (Thermo Scientific) and was calibrated against Pb-titrated Na_2S standards made in sulfide antioxidant buffer (SAOB).[29] Cell densities were estimated based on measurement of OD_{660} in 1 cm cuvets and calibration between OD_{660} and cell counts determined using a Coulter counter (Beckman Coulter Multisizer 4).[9]

2.5. Equilibrium Speciation Modeling. All equilibrium speciation modeling was performed in MINEQL+ v. 4.5 (Environmental Research Software). A detailed description of the assumptions and thermodynamic data used in the equilibrium speciation modeling are provided in the Supporting Information. Briefly, equilibrium constants for complexation of inorganic Hg(II) ($Hg(II)_i$) with sulfide were taken from Drott et al.,[30] including a revised value of the equilibrium constant for β-HgS(s) (metacinnabar) solubility. The equilibrium constant for $Hg(II)_i$ complexation by DOM thiols was taken from Skyllberg.[3] Thiol concentrations were estimated based on the measured S-to-C ratio in DOM samples and the percentage of total S as reduced exocyclic S. All other equilibrium constants were taken directly from the MINEQL+ database.

3. RESULTS AND DISCUSSION

3.1. Sulfur Incorporation into DOM. Reaction of Na_2S with DOM resulted in DOM with appreciably greater total S content (Figure 1a), although the yield of sulfurized DOM varied among the different DOM isolates. For SRHA and SRFA samples, S content increased from ~2−3 mmol S/mol C for unsulfurized DOM (slightly lower than IHSS's report of native S content of 4.14 and 3.15 mmol S/mol C for SRHA and SRFA, respectively; see Table 1) to ~6 mmol S/mol C at the highest added H_2S_T-to-DOC ratios. At the highest added H_2S_T-to-DOC ratios (40−50 mmol H_2S_T/mol C), less than 10% of added H_2S is incorporated into SRHA or SRFA, and sulfur incorporation plateaus at an addition of 20−30 mmol S/mol C. For the NLFA sample, total S content increased from 3.1 mmol S/mol C for unsulfurized DOM (3.3 mmol S/mol C reported by IHSS) to 12.8 mmol S/mol C. It is unclear whether the observed maximum S content of 12.8 mmol S/mol C represents the limit of total S incorporation for the NLFA sample, as a plateau in S incorporation was not obvious for this sample. Lastly, the PLFA sample, which had the highest native S content (measured as 11.0 mmol S/mol C; IHSS value = 21.7 mmol S/mol C), showed the lowest degree of S incorporation upon sulfide addition. While we obtained good agreement for total native S content for other samples with the reported IHSS elemental composition, our measure for native S content of PLFA was about 50% lower than the reported value. The proportion of S-containing molecules could be lower in our SPE-recovered DOM fraction compared to the original IHSS-isolated material. However, we have attempted to control for fractionation effects by comparing sulfurized DOM samples to unsulfurized samples having undergone the same SPE extraction and recovery procedure. We also note that for a given DOM sample, there was no relationship between S content and DOM recovery or DOM slope ratio (Table SI-1), suggesting that we extracted a similar DOM molecular fraction regardless of degree of sulfurization. The low extent of S incorporation for the PLFA sample may reflect the fact that this sample was already highly sulfurized prior to sulfide addition, and the finite sulfur incorporation capacity of the DOM had already been nearly reached. Sulfate reduction (as evidenced by H_2S odor and microbial species identified by 16S rRNA), which should enhance the sulfurization of DOM, is known to occur in Pony Lake.[31]

While there are clear differences in sulfur incorporation capacity among DOM samples, the chemical bases of these differences are not well-understood. Sulfurized OM can be produced by reactions of sulfide with ketones,[14] aldehydes,[14] carbohydrates,[32] quinones,[13] and other compounds containing one or more unsaturated carbon centers. For DOM, even when high-resolution MS data are available, we lack information regarding the structure and concentration of individual compounds that contribute to the DOM pool and must rely

DOI: 10.1021/acs.est.7b02781
Environ. Sci. Technol. XXXX, XXX, XXX−XXX

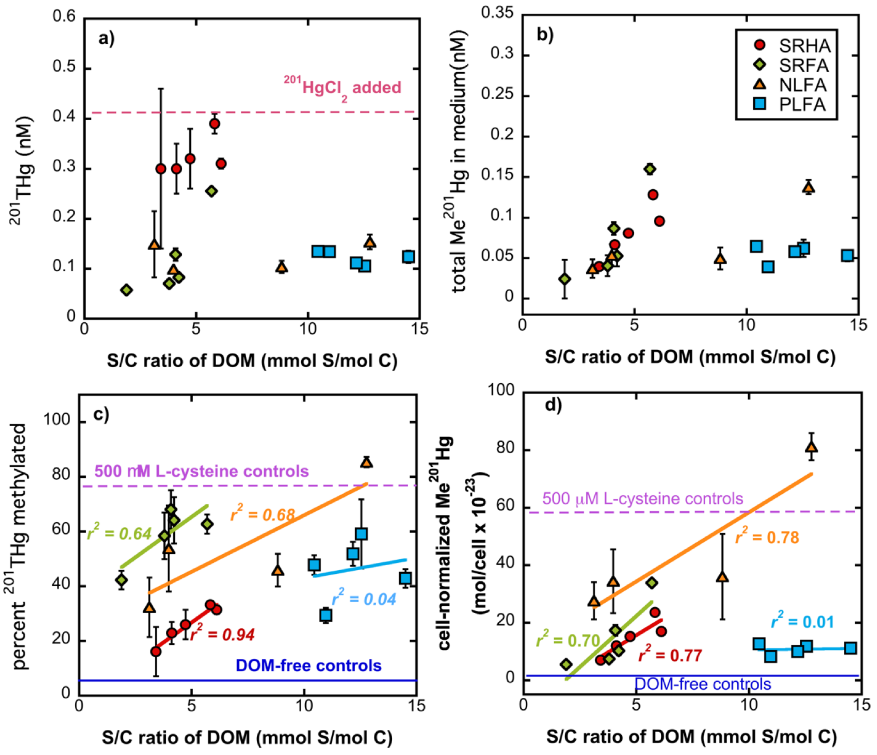

Figure 2. Methylmercury production by *Desulfovibrio desulfuricans* ND132 in Hg methylation assays as a function of the S-to-C ratio of dissolved organic matter. Methylation assays were conducted with 4.5 ± 1.6 × 10^8 cells/mL at pH 7.36 ± 0.15 and contained 8.3 to 10 mg C/L of DOM, and 3.4 ± 2.0 µM total sulfide (full details of experimental conditions are given in Table SI-3). (a) Total enriched ^{201}Hg in medium; (b) absolute production of enriched Me^{201}Hg; (c) fraction of total ^{201}Hg methylated; (d) cell-normalized Me^{201}Hg production. Shown in panels c and d are mean results for DOM-free controls and experiments with 500 µM L-cysteine for reference. Error bars are standard deviations of triplicate experiments, except for NLFA experiments that were performed in duplicate.

on bulk measures of DOM quality. One such measure is functional group content derived from ^{13}C NMR. Shown in Figure 1b, is the relationship between the sum of the percentage of carbonyl, carboxyl, and aromatic C and the S incorporation capacity. Here, S incorporation capacity is defined as the maximum observed S content (taken as the mean of the plateau in S content if evident; Figure 1a) following reaction with an excess of sulfide minus the native S content. Included in Figure 1b are data from Hoffmann et al.[16] and Poulin et al.,[20] for which both the S incorporation capacity of DOM and ^{13}C NMR data were reported or could be estimated. The data of Poulin et al.[20] are noteworthy for representing a "natural experiment" in which the S content of porewater DOM was measured along a natural porewater sulfide gradient in the Florida Everglades. The S incorporation capacities observed for the DOM samples employed in this study are consistent with that reported previously.[16,20] More interestingly, the proportion of carbonyl, carboxyl, and aromatic functional groups is a reasonably good predictor of susceptibility to abiotic S incorporation. The linear relationship between the summed percent carbonyl, carboxyl, and aromatic C and S incorporation capacity (r^2 = 0.86, p < 0.01) suggests that DOM quality, along with sulfide concentration, will play a role in the extent of DOM sulfurization during diagenesis. One caution regarding interpretation of Figure 1b is that our data set is dominated by DOM samples of terrestrial origin. Further work with DOM from autochthonous sources with a lower proportion of aromatic and carbonyl C[33] is needed to validate whether bulk measures of aromatic, carbonyl, and carboxyl functional-group content can be used to accurately predict DOM sulfur-incorporation capacity.

Our study did not include determination of S speciation in the sulfurized DOM. However, other work clearly shows that reduced S content of DOM increases approximately linearly with increased total S incorporation.[16,20] We thus have high confidence that total DOM S is a good proxy for reduced S functional groups important to Hg biogeochemistry.

3.2. Impact of DOM Sulfurization on Hg Methylation in Hg−DOM−Sulfide Solutions. As a case study for the importance of DOM sulfurization on trace element speciation and bioreactivity, we evaluated Hg methylation by *D. desulfuricans* ND132 in solutions containing ^{201}Hg(II)$_i$, sulfurized DOM, and low levels of sulfide (3.9 ± 2.2 µM across all experiments; see Table SI-4 for concentrations in individual experiments). Figure 2a shows total Hg concentration in the experiments as a function of the degree of sulfurization (expressed as S-to-C ratio of DOM) for each DOM sample. Significant (up to 75%) loss of the ^{201}HgCl$_2$ spike (dashed line in Figure 2a) is mostly attributed to ^{201}Hg(II)$_i$ sorption to polycarbonate sample containers during the pre-equilibration of the ^{201}HgCl$_2$ spike with DOM (or no DOM or 500 µM L-cysteine in controls) in the minimal medium. We confirmed this in a subset of experiments (with SRFA and PLFA) by directly measuring ^{201}Hg on bottle walls. This was done by adding 1% v/v BrCl + 1% v/v HCl directly to bottles used for pre-equilibrating ^{201}HgCl$_2$ with sulfurized DOM in the minimal medium to desorb ^{201}Hg from bottle walls. Accounting for ^{201}Hg(II)$_i$ recovered from bottle walls, we recovered a total of 81.9 ± 9.9% of total added ^{201}HgCl$_2$,

DOI: 10.1021/acs.est.7b02781
Environ. Sci. Technol. XXXX, XXX, XXX−XXX

similar to what we reported in previous studies.[8,9] The sorption is likely hydrophobic partitioning of neutral $Hg(SR)_2$ complexes onto the plastic bottle surfaces. Our recovery of sorbed Hg indicates that losses of ^{201}Hg due to reduction by DOM[34,35] and evasion of Hg(0) are not significant in these experiments. While the extent of $^{201}Hg(II)_i$ sorption to bottle walls varied among DOM samples, DOM sulfurization had minimal impact on the extent of bottle wall sorption, with the exception of the experiment with SRFA, for which we observed lower bottle wall sorption with increasing DOM sulfurization. Thus, the initial character of each DOM isolate had a larger impact on Hg sorption to bottle walls than did the extent of its sulfurization.

For all DOM samples, Hg methylation by strain ND132 in Hg-sulfide solutions was greater with DOM (range of 16.1−89.8% of ^{201}THg methylated) compared to DOM-free Hg−sulfide solutions (5.5 ± 5.3% ^{201}THg methylated; Figure 2c). A similar conclusion is reached when comparing cell-normalized MeHg production (Figure 2d; 5−80 × 10^{-23} mol/cell in DOM-containing solutions versus 1.1 ± 0.9 × 10^{-23} mol/cell in DOM-free experiments). A DOM-dependent enhancement in Hg methylation of 3- to 16-fold under mildly sulfidic conditions ($[H_2S]_T$ = 3.4 ± 1.6 μM) is consistent with previous findings with a chemically diverse suite of DOM isolates evaluated under similar conditions.[9] Interestingly, in some experiments with sulfurized DOM, Hg methylation efficiency (based on the percent ^{201}THg methylated) approaches, or even exceeds, that observed in positive controls with 500 μM L-cysteine (mean % MeHg of 79.7 ± 27.9%; Figure 2c), a ligand known to facilitate high rates of $Hg(II)_i$ biouptake in strain ND132[25,36] and other bacteria.[27,37] That similar efficiencies of Hg methylation (and, hence, bio-uptake) can be achieved in Hg−sulfide−DOM solutions highlights the magnitude of the DOM-dependent enhancement in $Hg(II)_i$ bioavailability.

For three out of four DOM samples evaluated (SRHA, SRFA, and NLFA), absolute MeHg production (Figure 2b), percent MeHg (^{201}THg as MeHg; Figure 2c), and cell-normalized MeHg production (Figure 2d) increase with increasing sulfurization of DOM. For these three isolates, percent MeHg was linearly correlated with the S-to-C ratio for each DOM sample (r^2 = 0.94 for SRHA, 0.64 for SRFA, and 0.68 for NLFA), and percent Hg methylation increased 1.5−3 fold upon additional DOM sulfur incorporation. For PLFA, which exhibited the smallest relative change in sulfur content upon reaction with sulfide (Figure 1), there was no significant effect of sulfurization on MeHg production by strain ND132 in DOM-sulfide solutions. In our previous work, we identified DOM sulfur content as a potentially important variable in controlling $Hg(II)_i$ bioavailability in Hg−sulfide−DOM solutions based on a multiple linear regression analysis of DOM properties versus Hg methylation.[9] Here, by directly modifying DOM sulfur content via low-temperature reaction with sulfide that mimics the diagenetic sulfurization of DOM, we directly confirm that DOM sulfur content contributes to the propensity of DOM to enhance Hg methylation in sulfidic solutions. In addition to the earlier study by Hoffmann et al. that showed increased arsenite sorption following DOM sulfurization,[16] our study is among the first to demonstrate the importance of DOM sulfurization to trace metal and metalloid fate.

3.3. Mechanisms of DOM-Enhanced Hg Methylation. DOM may enhance microbial Hg methylation by multiple causal mechanisms, including: (1) stimulation of microbial metabolism, (2) increasing cell membrane permeability to other solutes,[38] (3) inhibition of growth and aggregation of HgS(s) (metacinnabar)[4−7] with increased bioavailability of nanoscale HgS(s) relative to bulk HgS(s),[10,39,40] and (4) formation of specific $Hg(II)_i$−ligand complexes (e.g., $Hg(II)_i$−thiol complexes) with high bioavailability for uptake and subsequent methylation.[12] While all of these mechanisms may be operative concurrently, experimental evidence[8] suggests that stimulation of microbial metabolism and increased cell wall and membrane permeability are unimportant in these short-term experiments. Furthermore, DOM sulfurization is likely to increase DOM recalcitrance to microbial utilization (thus contributing to organic matter preservation in natural environments),[41] and it is unlikely that sulfurization would alter the surfactant-like properties of DOM critical to DOM accumulation at cell surfaces.[38] Thus, inhibition of HgS(s) growth and aggregation and high bioavailability of Hg−DOM thiol complexes are the most plausible explanations for increased Hg methylation in the presence of sulfurized DOM. We discuss each of these possibilities below.

Earlier work on metal sulfide dissolution[33] and precipitation/aggregation[4,42] emphasized the importance of nonspecific, steric interactions related to DOM aromaticity and molecular weight in controlling DOM's inhibition of metal sulfide precipitation and dissolution or enhancement of dissolution, but these studies were performed at high metal-to-DOM ratios at which contributions of low-abundance thiol moieties with well-documented impacts on metal sulfide growth and aggregation[5,43,44] may have been less-evident. Using the most recent thermodynamic data for metacinnabar solubility,[30] Hg−sulfide[30] and Hg−DOM thiol complexation[3] (summarized in Table SI-3), we predict metacinnabar precipitation in all experiments with SRHA and NLFA, some of the SRFA experiments, and none of the PLFA experiments, in which measured sulfide concentrations were greatest (Table SI-5). The solubility product for metacinnabar is a source of considerable uncertainty in this model,[45] and the log K_{sp} = 36.8 recommended by Drott et al.[30] is toward the lower end of the uncertainty range for log K_{sp} reported in the NIST Critical database (log K_{sp} = 38.0 ± 2.0).[46] A major obstacle to reliable measurement of β-HgS(s) solubility is distinguishing nanoparticulate Hg from truly dissolved Hg; Drott et al.[30] used 20 nm pore size filters in their determination of β-HgS(s) solubilty, but primary β-HgS(s) particles can be as small as 2−5 nm in diameter.[7,47] The inclusion of nanoparticulate β-HgS(s) in the dissolved fraction can lead to overestimates of β-HgS(s) solubility. Highlighting the sensitivity of the model results to the value of the metacinnabar solubility product, an increase in log K_{sp} from 36.8 to 38.0 results in predicted metacinnabar supersaturation across all experimental treatments. Given that Hg methylation increased with increasing DOM sulfurization under conditions of metacinnabar supersaturation, we posit that sulfurization has the same effect as increasing DOM concentration[8] on $Hg(II)_i$ bioavailability and that Hg methylation efficiency increases with an increasing DOM thiol-to-Hg molar ratio. Shown in Figure SI-1 are methylation efficiencies for sulfurized SRHA superimposed upon data for SRHA at various DOM-to-THg ratios from Graham et al.[8] When the DOM concentration is expressed as DOM thiol concentration (based on measured S-to-C ratio and the assumption that 23.6% of SRHA sulfur is as exocyclic S species), all of the SRHA data collapse onto a single line (slope = 0.57, r^2 = 0.89, p < 0.001). In our previous evaluation of Hg methylation in Hg−sulfide−DOM solutions, we noted that

DOI: 10.1021/acs.est.7b02781
Environ. Sci. Technol. XXXX, XXX, XXX−XXX

DOM S content was an important predictor of DOM's ability to enhance Hg methylation, and hypothesized that DOM thiols might act as capping agents preventing metacinnabar growth/aggregation.[9] Our direct manipulation of DOM thiol content confirms the important role of DOM thiols, even under conditions in which metacinnabar formation is likely and in which Hg−DOM thiol complexes are a small fraction (<0.01 to 2.4%; Table SI-5) of total $Hg(II)_i$. The exact mechanism of enhanced bioavailability of nanoscale HgS relative to bulk forms is unknown, but an increased rate of HgS dissolution and ligand exchange at the cell surface for nanoscale HgS capped by DOM thiols is one possibility. Biochemical pathways of $Hg(II)_i$ uptake by Hg-methylating bacteria are poorly understood, although essential trace metal transporters (e.g., for Zn) may be involved.[48]

An alternative hypothesis is that sulfurization of DOM increases the pool of $Hg(II)_i$−ligand complexes that are preferentially taken up by strain ND132. Past workers suggested that $Hg(II)_i$ bioavailability for methylation could be predicted by the concentration of neutral $Hg(II)_i$ species that are more readily taken up by bacteria via passive diffusion.[49−51] In this study, we observed no correlation between the predicted concentration of neutral $Hg(II)_i$ species and cell-normalized MeHg production (Figure SI-2a). Cell-normalized MeHg production was weakly negatively correlated (r^2 = 0.19, p = 0.06) with predicted total dissolved Hg concentration, suggesting that differences in metacinnabar solubility were not driving observed differences in MeHg production. As shown in Figure 3, a positive correlation is observed (r^2 = 0.54, p < 0.001), however, between the log of the predicted $Hg(SR)_2$ concentration and the log of cell-normalized MeHg production across all experiments. A pair of points are noteworthy about this observation. First, much (54%) of the variation in cell-normalized Hg methylation can be explained by the predicted $Hg(SR)_2$ concentration despite significant differences in DOM aromaticity, ^{201}THg concentration, cell density, and generally smaller differences in sulfide, pH, and DOM concentration across experiments. Second, data for Hg methylation by ND132 in the presence of 500 μM L-cysteine fall roughly along the regression line (slope of regression line decreases from 0.25 to 0.17 when including the cysteine data, r^2 increases to 0.64). Schaefer et al. observed similar rates of Hg methylation by ND132 in the presence of three thiol containing amino acids and peptides (cysteine, penicillamine, and glutathione).[36] Recently, Mazrui et al.,[12] in sediment microcosm experiments, demonstrated enhanced Hg methylation when sediments were amended with Hg−DOM complexes under conditions of undersaturation with respect to metacinnabar. These workers hypothesized either the direct uptake of Hg−-DOM complexes (presumably Hg−DOM thiol complexes) or DOM ligands acting as a shuttle between solution and the cell surface metal ion transporters hypothesized[48] to be involved in $Hg(II)_i$ uptake. Integrating these observations together with the data presented here, we can hypothesize that complexes of $Hg(II)_i$ with DOM thiols have similar bioavailability as $Hg(II)_i$ complexes with low-molecular-weight thiols such as cysteine. As noted above, Hg−DOM thiol complexes are predicted to be a small (<0.01 to 2.4%) fraction of the total Hg pool in these experiments, and predicted $Hg(SR)_2$ concentrations are in many cases several orders of magnitude smaller than observed MeHg concentrations (10^{-15}—10^{-12} M for $Hg(SR)_2$ versus 10^{-11}—10^{-10} M for MeHg). The concentration of available DOM thiols is predicted to be in large excess of $Hg(II)_i$ (see Table SI-4), however, allowing for continual $Hg(SR)_2$ complex formation with intracellular compartmentalization of $Hg(II)_i$ and subsequent methylation. The observed MeHg production could be driven by a small pool of highly bioavailable $Hg(SR)_2$ complexes if formation of new $Hg(SR)_2$ complexes to replace $Hg(SR)_2$ complexes taken up by cells is sufficiently rapid. Hg methylation efficiencies less than 100% may reflect competition between Hg internalization and methylation and sorption to the cell wall or membrane or other cellular components.[52] Several studies suggest that the equilibrium of $Hg(II)_i$ with strong S-donor ligands occurs on time scales of hours to days,[26,53] raising the possibility that rates of ligand exchange may play a role in microbial Hg methylation.[37,52]

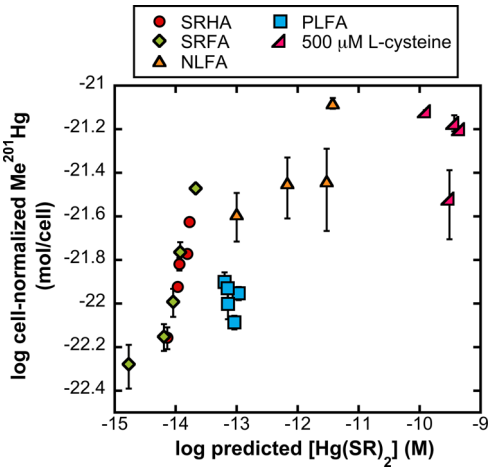

Figure 3. Relationship between the predicted concentration of $Hg(SR)_2$ complexes, where SR is an organic thiol (either DOM thiol or L-cysteine), and the cell-normalized MeHg production. Predicted $Hg(SR)_2$ concentrations at equilibrium were calculated based on experimental pH, estimated organic thiol concentration, total Hg concentration, and sulfide concentrations (see text and the Supporting Information for details).

To summarize, sulfurization of DOM clearly increases the bioavailability of $Hg(II)_i$ in Hg−sulfide−DOM solutions. A pair of plausible, nonmutually exclusive mechanisms for this increase in bioavailability are that DOM thiols stabilize HgS clusters and nanoparticles highly bioavailable for uptake and that DOM thiols form complexes with $Hg(II)_i$ directly taken up or readily exchanged on the cell surface. At present, we cannot clearly distinguish between these two mechanisms, in part because the low Hg concentrations necessary to mimic environmental conditions (and realistic Hg-to-DOM ratios) are inaccessible to direct spectroscopic investigation of $Hg(II)_i$ speciation. In either case, DOM sulfurization profoundly alters Hg uptake and methylation.

3.4. Environmental Implications. As demonstrated in this paper, DOM sulfurization can play an important role in the biogeochemical cycling of chalcophilic trace elements such as Hg. Increased DOM sulfurization leads to enhanced microbial production of the potent neurotoxin MeHg under conditions in which Hg−DOM thiol complexes are predicted to be only minor $Hg(II)_i$ species. While there have been significant advances in total thiol quantification in soil and sediment porewaters,[54] investigations of DOM composition using Fourier transform ion cyclotron resonance mass spectrometry[18−20] suggest that both the molecular diversity and concentration of DOM thiols in soils and sediment porewaters

DOI: 10.1021/acs.est.7b02781
Environ. Sci. Technol. XXXX, XXX, XXX−XXX

may be greater than previously realized. For example, in the highly eutrophied portions of the Northern Florida Everglades, where porewater sulfide concentrations can reach the several hundred micromolar level and DOC concentrations range from 40 to 100 mg/L, and porewater DOM thiols produced by sulfurization likely reach upward of 30 μM.[20] Interestingly, we also observed that organic matter that is more "terrestrial" in nature (higher aromaticity and average molecular weight) has greater capacity for sulfurization. While natural or anthropogenic sulfate enrichment of terrestrial ecosystems undoubtedly contributes to stimulation of sulfate-reducing bacteria, an important group of Hg methylators,[55] sulfurization of DOM may also enhance $Hg(II)_i$ bioavailability for methylation in such environments.

■ ASSOCIATED CONTENT

Supporting Information

The Supporting Information is available free of charge on the ACS Publications website at DOI: 10.1021/acs.est.7b02781.

Tables showing DOM recovery, quality assurance and control data, thermodynamic data, a summary of experimental variables, and results of equilibrium speciation modeling. Text describing the approach to equilibrium speciation modeling. Figures showing the relationships between the Hg-to-DOM thiol ratio and the fraction of Hg methylated and between Hg and cell-normalized MeHg production. (PDF)

■ AUTHOR INFORMATION

Corresponding Author

*Phone: 641-269-9813. E-mail: grahaman@grinnell.edu.

ORCID

Andrew M. Graham: 0000-0001-5189-6175

Notes

The authors declare no competing financial interest.

■ ACKNOWLEDGMENTS

We gratefully acknowledge support from the Grinnell College Mentored Advanced Project program and a National Science Foundation (NSF)-funded Research Experience for Undergraduates internship at the Smithsonian Environmental Research Center (SERC) awarded to K.C.B. SERC research was sponsored by the U.S. Department of Energy (DOE) Office of Science Biological and Environmental Research Subsurface Biogeochemical Research (SBR) Program through the Mercury Science Focus Area at Oak Ridge National Laboratory (ORNL) and by NIEHS award no. 1R01ES024284-01 to U. Ghosh, C. Gilmour, and D. Elias. Laboratory assistance was provided by Ally Bullock and Alyssa McBurney. The manuscript was improved thanks to useful comments from Brett Poulin.

■ REFERENCES

(1) Bergamaschi, B. A.; Krabbenhoft, D. P.; Aiken, G. R.; Patino, E.; Rumbold, D. G.; Orem, W. H. Tidally driven export of dissolved organic carbon, total mercury, and methylmercury from a mangrove-dominated estuary. *Environ. Sci. Technol.* **2012**, *46*, 1371−1378.

(2) Brigham, M. E.; Wentz, D. A.; Aiken, G. R.; Krabbenhoft, D. P. Mercury cycling in stream ecosystems. 1. Water column chemistry and transport. *Environ. Sci. Technol.* **2009**, *43*, 2720−2725.

(3) Skyllberg, U. Competition among thiols and inorganic sulfides and polysulfides for Hg and MeHg in wetland soils and sediments under suboxic conditions: Illumination of controversies and implications for MeHg net production. *J. Geophys Res-Biogeo* **2008**, *113*, G00C03.

(4) Ravichandran, M.; Aiken, G.; Ryan, J.; Reddy, M. Inhibition of precipitation and aggregation of metacinnabar (mercuric sulfide) by dissolved organic matter isolated from the Florida Everglades. *Environ. Sci. Technol.* **1999**, *33*, 1418−1423.

(5) Deonarine, A.; Hsu-Kim, H. Precipitation of mercuric sulfide nanoparticles in NOM-containing water: Implications for the natural environment. *Environ. Sci. Technol.* **2009**, *43*, 2368−2373.

(6) Slowey, A. J. Rate of formation and dissolution of mercury sulfide nanoparticles: The dual role of natural organic matter. *Geochim. Cosmochim. Acta* **2010**, *74*, 4693−4708.

(7) Gerbig, C.; Kim, C.; Stegemeier, J.; Ryan, J. N.; Aiken, G. R. Formation of nanocolloidal metacinnabar in mercury-DOM-sulfide systems. *Environ. Sci. Technol.* **2011**, *45*, 9180−9187.

(8) Graham, A. M.; Aiken, G. R.; Gilmour, C. C. Dissolved organic matter enhances microbial mercury methylation under sulfidic conditions. *Environ. Sci. Technol.* **2012**, *46*, 2715−2723.

(9) Graham, A. M.; Aiken, G. R.; Gilmour, C. C. Effect of dissolved organic matter source and character on microbial Hg methylation in Hg−S−DOM solutions. *Environ. Sci. Technol.* **2013**, *47* (11), 5746−5754.

(10) Zhang, T.; Kim, B.; Levard, C.; Reinsch, B. C.; Lowry, G. V.; Deshusses, M. A.; Hsu-Kim, H. Methylation of mercury by bacteria exposed to dissolved, nanoparticulate, and microparticulate mercuric sulfides. *Environ. Sci. Technol.* **2012**, *46*, 6950−6958.

(11) Chiasson-Gould, S. A.; Blais, J. M.; Poulain, A. J. Dissolved organic matter kinetically controls mercury bioavailability to bacteria. *Environ. Sci. Technol.* **2014**, *48*, 3153−3161.

(12) Mazrui, N. M.; Jonsson, S.; Thota, S.; Zhao, J.; Mason, R. P. Enhanced availability of mercury bound to dissolved organic matter for methylation in marine sediments. *Geochim. Cosmochim. Acta* **2016**, *194*, 153−162.

(13) Perlinger, J.; Kalluri, V.; Venkatapathy, R.; Angst, W. Addition of hydrogen sulfide to juglone. *Environ. Sci. Technol.* **2002**, *36*, 2663−2669.

(14) Schouten, S.; Vandriel, G. B.; Damste, J. S. S.; Deleeuw, J. W. Natural sulfurization of ketones and aldehydes - a key reaction in the formation of organic sulfur-compounds. *Geochim. Cosmochim. Acta* **1993**, *57*, 5111−5116.

(15) Heitmann, T.; Blodau, C. Oxidation and incorporation of hydrogen sulfide by dissolved organic matter. *Chem. Geol.* **2006**, *235*, 12−20.

(16) Hoffmann, M.; Mikutta, C.; Kretzschmar, R. Bisulfide reaction with natural organic matter enhances arsenite sorption: Insights from X-ray absorption spectroscopy. *Environ. Sci. Technol.* **2012**, *46*, 11788−11797.

(17) Yu, Z.-G.; Peiffer, S.; Göttlicher, J.; Knorr, K.-H. Electron transfer budgets and kinetics of abiotic oxidation and incorporation of aqueous sulfide by dissolved organic matter. *Environ. Sci. Technol.* **2015**, *49*, 5441−5449.

(18) Sleighter, R. L.; Chin, Y.-P.; Arnold, W. A.; Hatcher, P. G.; McCabe, A. J.; McAdams, B. C.; Wallace, G. C. Evidence of incorporation of abiotic S and N into prairie wetland dissolved organic matter. *Environ. Sci. Technol. Lett.* **2014**, *1*, 345−350.

(19) Hertkorn, N.; Harir, M.; Cawley, K. M.; Schmitt-Kopplin, P.; Jaffé, R. Molecular characterization of dissolved organic matter from subtropical wetlands: a comparative study through the analysis of optical properties, NMR and FTICR/MS. *Biogeosciences* **2016**, *13*, 2257−2277.

(20) Poulin, B. A.; Ryan, J. N.; Nagy, K. L.; Stubbins, A.; Dittmar, T.; Orem, W.; Krabbenhoft, D. P.; Aiken, G. R. Spatial dependence of reduced sulfur in Everglades dissolved organic matter controlled by sulfate enrichment. *Environ. Sci. Technol.* **2017**, *51*, 3630−3639.

(21) Manceau, A.; Nagy, K. L. Quantitative analysis of sulfur functional groups in natural organic matter by XANES spectroscopy. *Geochim. Cosmochim. Acta* **2012**, *99*, 206−223.

DOI: 10.1021/acs.est.7b02781
Environ. Sci. Technol. XXXX, XXX, XXX−XXX

(22) Dittmar, T.; Koch, B.; Hertkorn, N.; Kattner, G. A simple and efficient method for the solid-phase extraction of dissolved organic matter (SPE-DOM) from seawater. *Limnol. Oceanogr.: Methods* **2008**, *6*, 230−235.
(23) Helms, J. R.; Stubbins, A.; Ritchie, J. D.; Minor, E. C.; Kieber, D. J.; Mopper, K. Absorption spectral slopes and slope ratios as indicators of molecular weight, source, and photobleaching of chromophoric dissolved organic matter. *Limnol. Oceanogr.* **2008**, *53* (3), 955−969.
(24) Gilmour, C. C.; Elias, D. A.; Kucken, A. M.; Brown, S. D.; Palumbo, A. V.; Schadt, C. W.; Wall, J. D. Sulfate-reducing bacterium *Desulfovibrio desulfuricans* ND132 as a model for understanding bacterial mercury methylation. *Appl. Environ. Microb* **2011**, *77*, 3938−3951.
(25) Graham, A. M.; Bullock, A. L.; Maizel, A. C.; Elias, D. A.; Gilmour, C. C. A detailed assessment of the kinetics of Hg-cell association, Hg methylation, and MeHg degradation in several *Desulfovibrio* species. *Appl. Environ. Microb* **2012**, *78*, 7337−7346.
(26) Miller, C. L.; Southworth, G.; Brooks, S.; Liang, L.; Gu, B. Kinetic controls on the complexation between mercury and dissolved organic matter in a contaminated environment. *Environ. Sci. Technol.* **2009**, *43*, 8548−8553.
(27) Schaefer, J. K.; Morel, F. M. M. High methylation rates of mercury bound to cysteine by Geobacter sulfurreducens. *Nat. Geosci.* **2009**, *2*, 123−126.
(28) Hintelmann, H.; Ogrinc, N. Determination of stable mercury isotopes by ICP/MS and their application in environmental studies. In *Biogeochemistry of Environmentally Important Trace Metals*; Cai, Y., Braids, C. O., Eds.; American Chemical Society: Washington, DC, **2002**; pp *835*321−338.10.1021/bk-2003-0835.ch021
(29) Clesceri, L. S.; Greenberg, A. E.; Eaton, A. D. In *Standard Methods for the Examination of Water and Wastewater*; American Public Health Association: Washington, DC, 2000; pp 4−170−4−183.
(30) Drott, A.; Björn, E.; Bouchet, S.; Skyllberg, U. Refining thermodynamic constants for mercury(II)-sulfides in equilibrium with metacinnabar at sub-micromolar aqueous sulfide concentrations. *Environ. Sci. Technol.* **2013**, *47*, 4197−4203.
(31) Foreman, C. M.; Dieser, M.; Greenwood, M.; Cory, R. M.; Laybourn-Parry, J.; Lisle, J. T.; Jaros, C.; Miller, P. L.; Chin, Y.-P.; McKnight, D. M. When a habitat freezes solid: microorganisms over-winter within the ice column of a coastal Antarctic lake. *FEMS Microbiol. Ecol.* **2011**, *76*, 401−412.
(32) van Dongen, B. E.; Schouten, S.; Baas, M.; Geenevasen, J. A. J.; Sinninghe Damste, J. S. An experimental study of the low-temperature sulfurization of carbohydrates. *Org. Geochem.* **2003**, *34*, 1129−1144.
(33) Waples, J.; Nagy, K.; Aiken, G.; Ryan, J. Dissolution of cinnabar (HgS) in the presence of natural organic matter. *Geochim. Cosmochim. Acta* **2005**, *69*, 1575−1588.
(34) Gu, B.; Bian, Y.; Miller, C. L.; Dong, W.; Jiang, X.; Liang, L. Mercury reduction and complexation by natural organic matter in anoxic environments. *Proc. Natl. Acad. Sci. U. S. A.* **2011**, *108*, 1479−1483.
(35) Zheng, W.; Liang, L.; Gu, B. Mercury reduction and oxidation by reduced natural organic matter in anoxic environments. *Environ. Sci. Technol.* **2012**, *46*, 292−299.
(36) Schaefer, J. K.; Rocks, S. S.; Zheng, W.; Liang, L.; Gu, B.; Morel, F. M. M. Active transport, substrate specificity, and methylation of Hg(II) in anaerobic bacteria. *Proc. Natl. Acad. Sci. U. S. A.* **2011**, *108*, 8714−8719.
(37) Thomas, S. A.; Tong, T.; Gaillard, J.-F. Hg(II) bacterial biouptake: the role of anthropogenic and biogenic ligands present in solution and spectroscopic evidence of ligand exchange reactions at the cell surface. *Metallomics* **2014**, *6*, 2213−2222.
(38) Vigneault, B.; Percot, A.; Lafleur, M.; Campbell, P. G. C. Permeability changes in model and phytoplankton membranes in the presence of aquatic humic substances. *Environ. Sci. Technol.* **2000**, *34*, 3907−3913.
(39) Zhang, T.; Kucharzyk, K. H.; Kim, B.; Deshusses, M. A.; Hsu-Kim, H. Net methylation of mercury in estuarine sediment microcosms amended with dissolved, nanoparticulate, and micro-particulate mercuric sulfides. *Environ. Sci. Technol.* **2014**, *48*, 9133−9141.
(40) Jonsson, S.; Skyllberg, U.; Nilsson, M. B.; Lundberg, E.; Andersson, A.; Bjorn, E. Differentiated availability of geochemical mercury pools controls methylmercury levels in estuarine sediment and biota. *Nat. Commun.* **2014***5*, 4624−.10.1038/ncomms5624
(41) Amrani, A. Organosulfur compounds: Molecular and isotopic evolution from biota to oil and gas. *Annu. Rev. Earth Planet. Sci.* **2014**, *42*, 733−768.
(42) Deonarine, A.; Lau, B. L. T.; Aiken, G. R.; Ryan, J. N.; Hsu-Kim, H. Effects of humic substances on precipitation and aggregation of zinc sulfide nanoparticles. *Environ. Sci. Technol.* **2011**, *45*, 3217−3223.
(43) Lau, B. L. T.; Hsu-Kim, H. Precipitation and growth of zinc sulfide nanoparticles in the presence of thiol-containing natural organic ligands. *Environ. Sci. Technol.* **2008**, *42* (19), 7236−7241.
(44) Gondikas, A. P.; Jang, E. K.; Hsu-Kim, H. Influence of amino acids cysteine and serine on aggregation kinetics of zinc and mercury sulfide colloids. *J. Colloid Interface Sci.* **2010**, *347*, 167−171.
(45) Hsu-Kim, H.; Kucharzyk, K. H.; Zhang, T.; Deshusses, M. A. Mechanisms regulating mercury bioavailability for methylating micro-organisms in the aquatic environment: A Critical Review. *Environ. Sci. Technol.* **2013**, *47*, 2441−2456.
(46) National Institute of Standards and Technology. *NIST Critically Selected Stability Constants of Metal Complexes*; National Institute of Standards and Technology: Gaithersburg, MD, 2013.
(47) Pham, A. L.-T.; Morris, A.; Zhang, T.; Ticknor, J.; Levard, C.; Hsu-Kim, H. Precipitation of nanoscale mercuric sulfides in the presence of natural organic matter: Structural properties, aggregation, and biotransformation. *Geochim. Cosmochim. Acta* **2014**, *133*, 204−215.
(48) Szczuka, A.; Morel, F. M. M.; Schaefer, J. K. Effect of thiols, zinc, and redox conditions on Hg uptake in *Shewanella oneidensis*. *Environ. Sci. Technol.* **2015**, *49*, 7432−7438.
(49) Mason, R.; Reinfelder, J.; Morel, F. Uptake, toxicity, and trophic transfer of mercury in a coastal diatom. *Environ. Sci. Technol.* **1996**, *30*, 1835−1845.
(50) Benoit, J.; Gilmour, C.; Mason, R. Aspects of bioavailability of mercury for methylation in pure cultures of Desulfobulbus propionicus (1pr3). *Appl. Environ. Microb* **2001**, *67*, 51−58.
(51) Drott, A.; Lambertsson, L.; Bjorn, E.; Skyllberg, U. Importance of dissolved neutral mercury sulfides for methyl mercury production in contaminated sediments. *Environ. Sci. Technol.* **2007**, *41*, 2270−2276.
(52) Liu, Y.-R.; Lu, X.; Zhao, L.; An, J.; He, J.-Z.; Pierce, E. M.; Johs, A.; Gu, B. Effects of cellular sorption on mercury bioavailability and methylmercury production by *Desulfovibrio desulfuricans* ND132. *Environ. Sci. Technol.* **2016**, *50*, 13335−13341.
(53) Miller, C. L.; Liang, L.; Gu, B. Competitive ligand exchange reveals time dependant changes in the reactivity of Hg-dissolved organic matter complexes. *Environ. Chem.* **2012**, *9*, 495.
(54) Liem-Nguyen, V.; Bouchet, S.; Bjorn, E. Determination of sub-nanomolar levels of low molecular mass thiols in natural waters by liquid chromatography tandem mass spectrometry after derivatization with p-(hydroxymercuri) benzoate and online preconcentration. *Anal. Chem.* **2015**, *87*, 1089−1096.
(55) Gilmour, C. C.; Podar, M.; Bullock, A. L.; Graham, A. M.; Brown, S. D.; Somenahally, A. C.; Johs, A.; Hurt, R. A., Jr.; Bailey, K. L.; Elias, D. A. Mercury methylation by novel microorganisms from new environments. *Environ. Sci. Technol.* **2013**, *47*, 11810−11820.

DOI: 10.1021/acs.est.7b02781
Environ. Sci. Technol. XXXX, XXX, XXX−XXX

Supporting Information
to
Sulfurization of Dissolved Organic Matter Increases Hg-S-DOM Bioavailability to a Hg-Methylating Bacterium

Andrew M. Graham[a*], Keaton Cameron-Burr[a], Hayley A. Hajic[a], Connie PS Lee[a], Deborah Msekela[a], and Cynthia C. Gilmour[b]

[a]Grinnell College Department of Chemistry, 1116 8th Ave, Grinnell, IA USA 50112
[b]Smithsonian Environmental Research Center, 647 Contees Wharf Rd, Edgewater, MD USA 21037
[*]Corresponding author, phone: 641-269-9813, email: grahaman@grinnell.edu

Contents:

Table SI-1. Recovery and UV-VIS spectral characteristics of sulfurized DOM by solid phase extraction (SPE). Slope ratio (S_R) is the ratio of the slope of the natural log transformed spectra in the wavelength range 275-295 nm divided by the slope in the range 350-400 nm. S_R is strongly correlated with the size and aromaticity of DOM as described in Helms et al. (2008).[1] The reported error on S_R was determined based on the relative standard errors of the linear fits to the natural log transformed spectra in each wavelength range.

Sample	Measured S/C ratio	SPE Recovery (%)	S_R (slope ratio)
SRHA (unsulfurized)	3.42	33.3	0.67±0.02
SRHA	4.12	34.6	0.67±0.02
SRHA	4.73	34.8	0.68±0.02
SRHA	6.12	32.8	0.66±0.02
SRHA	5.83	31.6	0.70±0.02
IHSS SRHA (no SPE)	not measured	not applicable	0.65±0.02
SRFA (unsulfurized)	1.88	67.3	0.69±0.02
SRFA	3.80	54.2	0.72±0.02
SRFA	4.22	53.5	0.69±0.02
SRFA	4.08	55.8	0.63±0.02
SRFA	5.69	52.5	0.70±0.02
IHSS SRFA (no SPE)	not measured	not applicable	0.82±0.05
NLFA (unsulfurized)	3.12	46.2	0.78±0.06
NLFA	3.98	46.6	0.76±0.06
NLFA	8.83	29.4	0.74±0.09
NLFA	12.8	44.9	0.84±0.05
IHSS NLFA (no SPE)	not measured	not applicable	0.65±0.04
PLFA (unsulfurized)	11.0	78.6	0.99±0.08
PLFA	10.4	75.6	0.79±0.06
PLFA	14.5	75.0	0.76±0.05
PLFA	12.5	79.9	0.85±0.06
PLFA	12.2	81.3	0.96±0.09
IHSS PLFA (no SPE)	not measured	not applicable	0.91±0.06

Table SI-2. Quality control data for total Hg (THg) and methylmercury (MeHg) analyses. Instrument detection limit determined as three times standard deviation of blank.

Parameter	***Result***
$Me^{201}Hg$ instrument detection limit	0.11±0.18 pg (0.02 ng/L for 5 mL sample)
Distillation blanks for $Me^{201}Hg$	0.02±0.02 ng/L
Relative percent difference for duplicate MeHg analyses	7.4±6.2% (*n* = 5 pairs)
MeHg recovery for NIST 1566b (oyster tissue)	139±8% (*n* = 6 determinations)
^{201}THg instrument detection limit	0.37±0.38 ng/L
Digestion blanks for ^{201}Hg	0.02±0.04 ng/L
Relative percent difference for duplicate THg analyses	5.4±2.7% (*n* = 4 pairs)
THg recovery for NIST 2709a (San Joaquin soil)	91.6±22.0% (*n* = 8 determinations*)*

Instrument detection limit calculated as three times the standard deviation of reagent blanks.

Description of Equilibrium Speciation Modeling

Equilibrium speciation modeling was performed in MINEQL+ v. 4.6 (Environmental Research Software). Equilibrium constants were critically selected using the most up to date information on $Hg(II)_i$ complexation in natural waters. The solubility product for metacinnabar (HgS(s)) was recently reevaluated by Drott *et al.*[2] and reported as log K = 36.8, 1.2 log units lower than that reported in the NIST Critical Database.[3] Following Skyllberg,[4] we have assumed that $Hg(II)_i$ forms linear two-coordinate complexes with DOM thiols with a log K = 42.0. In this approach, we ignore the contribution of weaker O- and N- donor ligands in the DOM pool. This approach is justified for two reasons: 1) DOM/Hg ratios are sufficiently high in these experiments, such that binding will be dominated by stronger S-donor ligands[5]; 2) All solutions contain µM concentrations of sulfide further diminishing the contributions of weak $Hg(II)_i$-binding ligands. $[RSH]_T$ was estimated based upon [DOC], the measured S/C ratio, and the assumption that strong Hg(II)-binding thiols could be estimated based on the concentration of exocyclic sulfur in each DOM sample. Manceau and Nagy[6] determined S speciation using X-ray absorption near edge spectroscopy (XANES) for 3 out of the 4 isolates used in this study (and S speciation for the humic acid fraction of the Nordic Lake sample). The percentage of total S as reduced exocyclic S ranged from 23.6 to 46.9% (mean = 32.2±10.5%). We further assume that DOM S speciation is independent of total S content – recent data from Hoffmann *et al.*[7]and Poulin et al.[8] suggests, however, that the fraction of total S in reduced forms increases with increasing sulfurization. In that case, our application of a single conversion factor for total S to reduced S may underestimate the true contribution of DOM thiols to $Hg(II)_i$ binding. Other input parameters for modeling can be found in Table SI-3 below; for sulfide concentration, the mean of initial and final (t=3 h) concentrations were input into the speciation model. In modeling Hg-cysteine complexation, some reports suggest the possibility of a tris Hg(cys) complex (likely $Hg(Hcys)_3^-$.[9] Unfortunately, no thermodynamic data are available for this purported complex. Kõszegi-Szalai and Paál[10] reported equilibrium constants for Hg-penicillamine complexes, including a $Hg(Hpen)_3^-$ complex with a log K of 75.3 at I = 0 M. Given their similar structures (differing only in the two CH_3—substituents at the 3-position for penicillamine), we can evaluate the potential contributions of a $Hg(Hcys)_3^-$ complex to $Hg(II)_i$ speciation using the log K for the $Hg(Hgpen)_3^-$ complex. Using this approach, we find that $Hg(Hcys)_3^-$ is not likely to be a significant species under our experimental conditions ($[^{201}THg]$, $[H_2S]_T$, $[cys]_T$, and pH), and we do not include this species in our modeling. A summary of important thermodynamic data for speciation modeling can be found in Table SI-3 below.

Table SI-3. Thermodynamic data for equilibrium speciation modeling. Equilibrium constants for Hg-Cl and Hg-OH complexes were taken directly from the MINEQL+ database.

Reaction	***log K***	***Reference***
Hg-sulfide Aqueous Speciation		
$Hg^{2+} + 2HS^- = Hg(SH)_2^0$	39.1	Drott *et al.*[2]
$Hg^{2+} + 2HS^- = HgS_2H^- + H^+$	32.5	Drott *et al.*[2]
$Hg^{2+} + 2HS^- = HgS_2^{2-} + 2H^+$	23.2	Drott *et al.*[2]
Metacinnabar Precipitation		
$Hg^{2+} + HS^- = HgS(s) + H^+$	36.8	Drott *et al.*[2]
Hg-DOM Complexation		
$Hg^{2+} + 2RS^- = Hg(SR)_2$	42.0	Skyllberg[4]
$RS^- + H^+ = RSH$	10.0	Skyllberg[4]
Hg-CYS Complexation		
$Hg^{2+} + 2H^+ + 2CYS^{2-} = Hg(HCYS)_2^0$	64.1	Starý and Kratzer.[11]
$Hg^{2+} + 2CYS^{2-} = Hg(CYS)_2^{2-}$	43.9	Starý and Kratzer.[11]

Table SI-4. Summary of experimental variables in Hg methylation assays with *Desulfovibrio desulfuricans* ND132 in the presences of sulfurized DOM samples. DOM isolates were sulfurized as described in the main text, resulting in the S/C ratios reported in the table below. Reported values are means and standard deviations (*n* =3, excepting NLFA experiments, where *n* =2). n.d. = not determined due to lost samples. Cell density is average cell density measured at beginning and end of 3h incubation which typically increased less than 5% over the duration of the experiment.

DOM Isolate or Control	[DOC] (mg/L)	Measured S/C ratio (mmol S/mol C)	Cell density (x 10^8 cells/mL)	pH	Initial sulfide (µM)	Final sulfide (µM)	Total ^{201}Hg in medium (nM)	Total filterable ^{201}Hg (nM)	Total $Me^{201}Hg$ in medium (pM)
SRHA	9.19	3.42	5.68±0.21	7.27±0.01	2.25±0.05	3.62±0.12	0.30±0.16	0.21±0.01	39.6±4.9
SRHA	9.52	4.12	5.57±0.22	7.31±0.01	2.67±0.26	3.92±0.02	0.30±0.05	0.29±0.04	66.4±1.3
SRHA	9.58	4.73	5.32±0.31	7.25±0.01	3.36±0.08	4.15±0.11	0.32±0.06	0.26±0.04	80.7±1.5
SRHA	9.59	6.12	5.67±0.19	7.20±0.01	4.18±0.24	4.40±0.06	0.31±0.01	0.23±0.004	95.8±1.2
SRHA	9.24	5.83	5.43±0.09	7.33±0.02	3.72±0.17	4.53±0.10	0.39±0.02	0.24±0.01	128.4±1.9
SRFA	10	1.88	4.55±0.82	7.28±0.04	2.33±0.10	3.01±0.29	0.057±0.003	0.028±0.004	24.0±0.6
SRFA	10	3.80	5.75±1.51	7.28±0.04	2.79±0.29	3.22±0.20	0.070±0.008	0.034±0.007	40.5±1.6
SRFA	10	4.22	5.15±0.38	7.29±0.02	2.88±0.10	3.36±0.06	0.083±0.007	0.054±0.014	52.5±2.9
SRFA	10	4.08	5.03±0.52	7.22±0.02	2.87±0.03	3.44±0.14	0.13±0.01	0.088±0.007	86.6±0.2
SRFA	10	5.69	4.74±0.26	7.26±0.02	3.58±0.25	3.76±0.20	0.26±0.001	0.12±0.02	160±8
NLFA	10	3.12	1.44±0.21	7.52±0.12	0.26±0.18	0.95±0.83	0.15±0.07	0.067±0.006	36.9±11.4
NLFA	10	3.98	1.50±0.15	7.74±0.05	0.10±0.04	0.33±0.06	0.099±0.003	0.086±0.006	53.4±13.6
NLFA	10	8.83	1.36±0.18	7.61±0.10	0.05±0.01	0.42±0.31	0.10±0.01	0.090±0.01	49.5±13.4
NLFA	10	12.8	1.66±0.07	7.66±0.04	0.30±0.06	0.42±0.11	0.15±0.01	0.17±0.01	138±9
PLFA	8.3	11.0	4.79±0.23	7.35±0.02	3.99±0.27	6.44±0.78	0.13±0.004	0.018±0.002	39.2±4.0
PLFA	8.3	10.4	5.11±0.45	7.35±0.05	5.13±0.52	6.87±0.47	0.13±0.003	0.036±0.006	64.2±6.3
PLFA	8.3	14.5	4.76±0.33	7.34±0.05	5.13±0.52	7.02±0.28	0.12±0.01	0.038±0.002	53.0±7.0
PLFA	8.3	12.5	5.28±0.37	7.28±0.06	4.78±0.19	6.72±0.54	0.11±0.01	0.030±0.008	62.1±10.7
PLFA	8.3	12.2	5.80±0.89	7.32±0.02	5.13±0.52	6.56±0.26	0.11±0.01	0.049±0.008	57.8±0.8
500 µM L-cysteine control (SRHA)	N/A	N/A	5.74±0.13	7.28±0.00	5.78±0.11	19.3±0.1	0.46±0.02	0.07±0.01	362±6
500 µM L-cysteine control (SRFA)	N/A	N/A	4.04±0.67	7.14±0.00	5.55±0.72	31.1±4.9	0.37±0.02	0.28±0.02	308±11
500 µM L-cysteine control (NLFA)	N/A	N/A	1.43±0.17	7.30±0.06	0.28±0.10	4.08±3.1	0.13±0.02	n.d.	43.4±13.4
500 µM L-cysteine control (PLFA)	N/A	N/A	5.15±0.45	7.23±0.04	5.90±0.88	17.0±0.7	0.31±0.07	0.39±0.01	347±20
No DOM control (SRHA)	N/A	N/A	5.31±0.34	7.40±0.01	3.64±0.13	2.75±0.1	0.28±0.02	0.25±0.01	2.2±0.2
No DOM control (SRFA)	N/A	N/A	3.81±0.10	7.20±0.12	2.74±0.25	3.22±0.53	0.064±0.007	0.007±0.005	6.5±1.2

Table SI-5. Predicted equilibrium speciation of inorganic Hg(II) based on measured total ^{201}Hg in medium, pH, sulfide, DOC, and S/C ratio of DOM. $Hg(SR)_2$ is a two-coordinate complex of $Hg(II)_i$ with organic thiols; $Hg(SH)_2$ is the equivalent complex with inorganic sulfide.

DOM Isolate or Control	$[RSH]_T$ (μM)	[Meta-cinnabar] (M)	$[Hg(SR)_2]$ (M)	$[Hg(SH)_2]$ (M)	$[HgS_2H^-] + [HgS_2^{2-}]$ (M)	Total dissolved Hg (M)
SRHA	0.62	1.77×10^{-10}	7.28×10^{-15}	1.65×10^{-11}	1.06×10^{-10}	1.23×10^{-10}
SRHA	0.77	1.60×10^{-10}	1.08×10^{-14}	1.74×10^{-11}	1.23×10^{-10}	1.40×10^{-10}
SRHA	0.89	1.65×10^{-10}	1.15×10^{-14}	2.18×10^{-11}	1.33×10^{-10}	1.55×10^{-10}
SRHA	1.15	1.36×10^{-10}	1.55×10^{-14}	2.69×10^{-11}	1.47×10^{-10}	1.74×10^{-10}
SRHA	1.06	2.14×10^{-10}	1.69×10^{-14}	2.10×10^{-11}	1.55×10^{-10}	1.76×10^{-10}
SRFA	0.40	undersaturated	1.70×10^{-15}	7.50×10^{-12}	4.94×10^{-11}	5.69×10^{-11}
SRFA	0.80	undersaturated	6.44×10^{-15}	9.24×10^{-12}	6.09×10^{-11}	7.01×10^{-11}
SRFA	0.88	undersaturated	9.12×10^{-15}	1.07×10^{-11}	7.18×10^{-11}	8.25×10^{-11}
SRFA	0.85	undersaturated	1.19×10^{-14}	1.90×10^{-11}	1.09×10^{-10}	1.28×10^{-10}
SRFA	1.19	1.02×10^{-10}	2.13×10^{-14}	2.10×10^{-11}	1.32×10^{-10}	1.53×10^{-10}
NLFA	0.84	1.21×10^{-10}	1.00×10^{-13}	2.18×10^{-12}	2.54×10^{-11}	2.77×10^{-11}
NLFA	1.06	8.73×10^{-11}	6.80×10^{-13}	5.20×10^{-13}	1.03×10^{-11}	1.15×10^{-11}
NLFA	2.36	9.30×10^{-11}	3.00×10^{-12}	5.81×10^{-13}	8.42×10^{-12}	1.20×10^{-11}
NLFA	3.42	1.32×10^{-10}	3.77×10^{-12}	9.70×10^{-13}	1.59×10^{-11}	2.06×10^{-11}
PLFA	3.55	undersaturated	9.18×10^{-14}	1.53×10^{-11}	1.19×10^{-10}	1.34×10^{-10}
PLFA	3.39	undersaturated	6.34×10^{-14}	1.53×10^{-11}	1.19×10^{-10}	1.35×10^{-10}
PLFA	4.70	undersaturated	1.08×10^{-13}	1.44×10^{-11}	1.09×10^{-10}	1.24×10^{-10}
PLFA	5.75	undersaturated	7.14×10^{-14}	1.38×10^{-11}	9.11×10^{-11}	1.05×10^{-10}
PLFA	5.85	undersaturated	7.21×10^{-14}	1.35×10^{-11}	9.74×10^{-11}	1.11×10^{-10}
500 μM L-cysteine control (SRHA)	500	undersaturated	4.60×10^{-10}	2.43×10^{-19}	1.68×10^{-14}	4.60×10^{-10}
500 μM L-cysteine control (SRFA)	500	undersaturated	1.27×10^{-10}	7.12×10^{-17}	9.94×10^{-15}	1.27×10^{-10}
500 μM L-cysteine control (NLFA)	500	undersaturated	3.09×10^{-10}	6.09×10^{-17}	3.56×10^{-16}	3.09×10^{-10}
500 μM L-cysteine control (PLFA)	500	undersaturated	3.71×10^{-10}	2.59×10^{-15}	1.23×10^{-14}	3.71×10^{-10}
No DOM control (SRHA)	0	1.33×10^{-10}	0	1.44×10^{-11}	1.26×10^{-10}	1.40×10^{-10}
No DOM control (SRFA)	0	undersaturated	0	9.91×10^{-12}	5.41×10^{-11}	6.40×10^{-11}

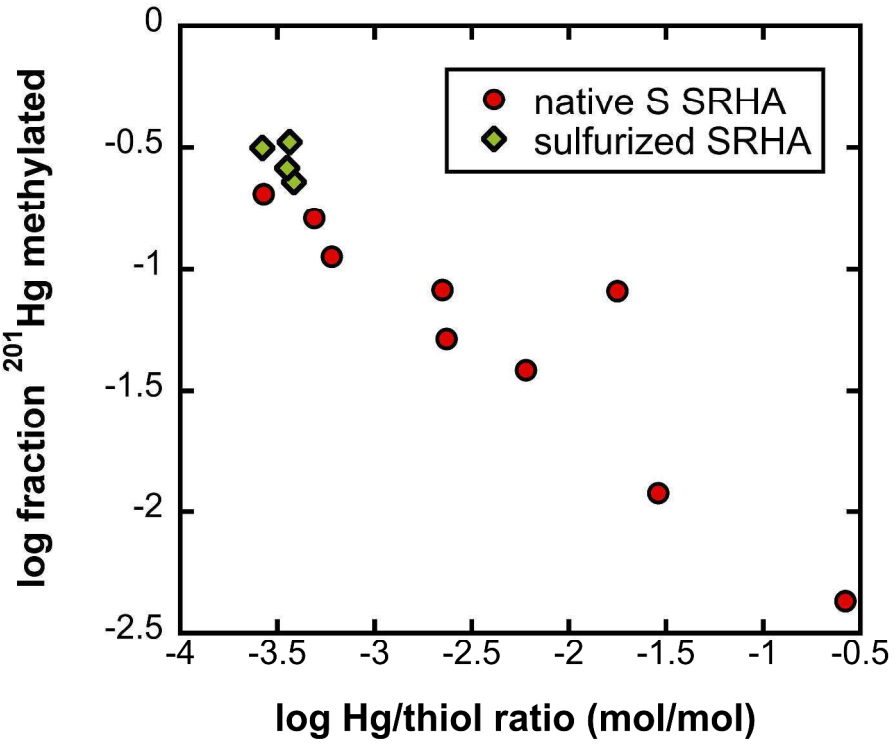

Figure SI-1. Relationship between log Hg/thiol ratio and log fraction ^{201}Hg methylated in solutions containing Suwannee River humic acid (SRHA), sulfide, and $^{201}HgCl_2$. Data for native SRHA include data from this study and from Graham et al.[12] Data for sulfurized SRHA from this study only. Thiol concentrations were estimated based on measured S/C ratio for SRHA samples and the assumption that 70% of total DOM S was thiols.

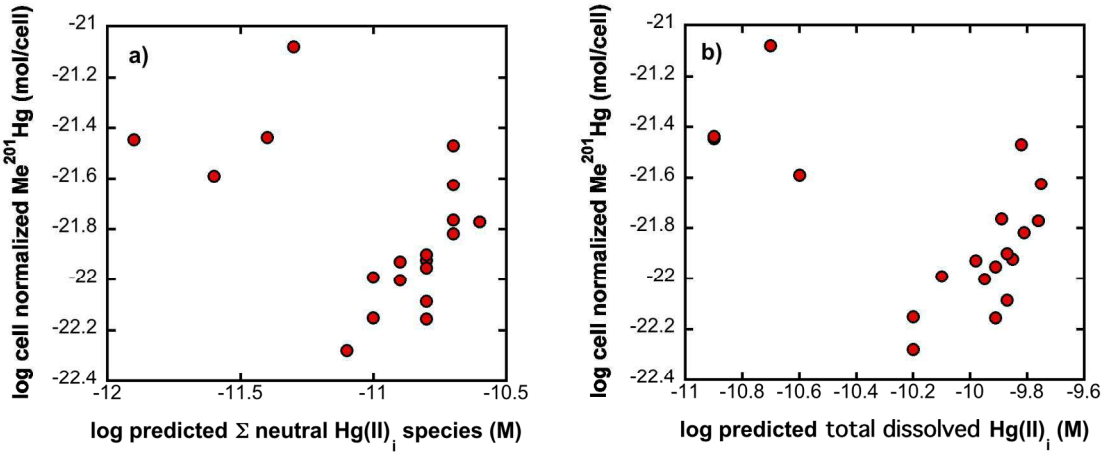

Figure SI-2. Correlations between the sum of neutral $Hg(II)_i$ species (**panel a**) or total dissolved $Hg(II)_i$ (**panel b**) and cell-normalized MeHg production. MeHg production cell-normalized due to significant differences in cell density between experiments. Data log-transformed due to non-normal distributions.

References for Supporting Information

1. Helms, J. R. *et al.* Absorption spectral slopes and slope ratios as indicators of molecular weight, source, and photobleaching of chromophoric dissolved organic matter. *Limnol Oceanogr* **53,** 955–969 (2008).
2. Drott, A., Björn, E., Bouchet, S. & Skyllberg, U. Refining thermodynamic constants for mercury(II)-sulfides in equilibrium with metacinnabar at sub-micromolar aqueous sulfide concentrations. *Environ Sci Technol* **47,** 4197–4203 (2013).
3. National Institute of Standards and Technology. NIST Critically Selected Stability Constants of Metal Complexes.
4. Skyllberg, U. Competition among thiols and inorganic sulfides and polysulfides for Hg and MeHg in wetland soils and sediments under suboxic conditions: Illumination of controversies and implications for MeHg net production. *J Geophys Res-Biogeo* **113,** G00C03 (2008).
5. Haitzer, M., Aiken, G. & Ryan, J. Binding of mercury(II) to dissolved organic matter: The role of the mercury-to-DOM concentration ratio. *Environ Sci Technol* **36,** 3564–3570 (2002).
6. Manceau, A. & Nagy, K. L. Quantitative analysis of sulfur functional groups in natural organic matter by XANES spectroscopy. *Geochim Cosmochim Acta* **99,** 206–223 (2012).
7. Hoffmann, M., Mikutta, C. & Kretzschmar, R. Bisulfide reaction with natural organic matter enhances arsenite sorption: Insights from X-ray absorption spectroscopy. *Environ Sci Technol* **46,** 11788–11797 (2012).
8. Poulin, B. A. *et al.* Spatial dependence of reduced sulfur in Everglades dissolved organic matter controlled by sulfate enrichment. *Environ Sci Technol* **51**, 3630-3639 (2017).
9. Schaefer, J. K. & Morel, F. M. M. High methylation rates of mercury bound to cysteine by Geobacter sulfurreducens. *Nature Geoscience* **2,** 123–126 (2009).
10. Koszegi-Szalai, H. & Paal, T. L. Equilibrium studies of mercury (II) complexes with penicillamine. *Talanta* **48,** 393–402 (1999).
11. Stary, J. & Kratzer, K. Radiometric determination of stability-constants of mercury species complexes with L-cysteine. *J Radioan Nucl Ch Le* **126,** 69–75 (1988).
12. Graham, A. M., Aiken, G. R. & Gilmour, C. C. Dissolved organic matter enhances microbial mercury methylation under sulfidic conditions. *Environ Sci Technol* **46,** 2715–2723 (2012).

Supporting Information
to
Sulfurization of Dissolved Organic Matter Increases Hg-S-DOM Bioavailability to a Hg-Methylating Bacterium

Andrew M. Graham[a*], Keaton Cameron-Burr[a], Hayley A. Hajic[a], Connie PS Lee[a], Deborah Msekela[a], and Cynthia C. Gilmour[b]

[a]Grinnell College Department of Chemistry, 1116 8th Ave, Grinnell, IA USA 50112
[b]Smithsonian Environmental Research Center, 647 Contees Wharf Rd, Edgewater, MD USA 21037
[*]Corresponding author, phone: 641-269-9813, email: grahaman@grinnell.edu

Contents:

Table SI-1. Recovery and UV-VIS spectral characteristics of sulfurized DOM by solid phase extraction (SPE). Slope ratio (S_R) is the ratio of the slope of the natural log transformed spectra in the wavelength range 275-295 nm divided by the slope in the range 350-400 nm. S_R is strongly correlated with the size and aromaticity of DOM as described in Helms et al. (2008).[1] The reported error on S_R was determined based on the relative standard errors of the linear fits to the natural log transformed spectra in each wavelength range.

Sample	Measured S/C ratio	SPE Recovery (%)	S_R (slope ratio)
SRHA (unsulfurized)	3.42	33.3	0.67±0.02
SRHA	4.12	34.6	0.67±0.02
SRHA	4.73	34.8	0.68±0.02
SRHA	6.12	32.8	0.66±0.02
SRHA	5.83	31.6	0.70±0.02
IHSS SRHA (no SPE)	not measured	not applicable	0.65±0.02
SRFA (unsulfurized)	1.88	67.3	0.69±0.02
SRFA	3.80	54.2	0.72±0.02
SRFA	4.22	53.5	0.69±0.02
SRFA	4.08	55.8	0.63±0.02
SRFA	5.69	52.5	0.70±0.02
IHSS SRFA (no SPE)	not measured	not applicable	0.82±0.05
NLFA (unsulfurized)	3.12	46.2	0.78±0.06
NLFA	3.98	46.6	0.76±0.06
NLFA	8.83	29.4	0.74±0.09
NLFA	12.8	44.9	0.84±0.05
IHSS NLFA (no SPE)	not measured	not applicable	0.65±0.04
PLFA (unsulfurized)	11.0	78.6	0.99±0.08
PLFA	10.4	75.6	0.79±0.06
PLFA	14.5	75.0	0.76±0.05
PLFA	12.5	79.9	0.85±0.06
PLFA	12.2	81.3	0.96±0.09
IHSS PLFA (no SPE)	not measured	not applicable	0.91±0.06

Table SI-2. Quality control data for total Hg (THg) and methylmercury (MeHg) analyses. Instrument detection limit determined as three times standard deviation of blank.

Parameter	***Result***
$Me^{201}Hg$ instrument detection limit	0.11±0.18 pg (0.02 ng/L for 5 mL sample)
Distillation blanks for $Me^{201}Hg$	0.02±0.02 ng/L
Relative percent difference for duplicate MeHg analyses	7.4±6.2% (*n* = 5 pairs)
MeHg recovery for NIST 1566b (oyster tissue)	139±8% (*n* = 6 determinations)
^{201}THg instrument detection limit	0.37±0.38 ng/L
Digestion blanks for ^{201}Hg	0.02±0.04 ng/L
Relative percent difference for duplicate THg analyses	5.4±2.7% (*n* = 4 pairs)
THg recovery for NIST 2709a (San Joaquin soil)	91.6±22.0% (*n* = 8 determinations*)*

Instrument detection limit calculated as three times the standard deviation of reagent blanks.

Description of Equilibrium Speciation Modeling

Equilibrium speciation modeling was performed in MINEQL+ v. 4.6 (Environmental Research Software). Equilibrium constants were critically selected using the most up to date information on $Hg(II)_i$ complexation in natural waters. The solubility product for metacinnabar (HgS(s)) was recently reevaluated by Drott *et al.*[2] and reported as log K = 36.8, 1.2 log units lower than that reported in the NIST Critical Database.[3] Following Skyllberg,[4] we have assumed that $Hg(II)_i$ forms linear two-coordinate complexes with DOM thiols with a log K = 42.0. In this approach, we ignore the contribution of weaker O- and N- donor ligands in the DOM pool. This approach is justified for two reasons: 1) DOM/Hg ratios are sufficiently high in these experiments, such that binding will be dominated by stronger S-donor ligands[5]; 2) All solutions contain µM concentrations of sulfide further diminishing the contributions of weak $Hg(II)_i$-binding ligands. $[RSH]_T$ was estimated based upon [DOC], the measured S/C ratio, and the assumption that strong Hg(II)-binding thiols could be estimated based on the concentration of exocyclic sulfur in each DOM sample. Manceau and Nagy[6] determined S speciation using X-ray absorption near edge spectroscopy (XANES) for 3 out of the 4 isolates used in this study (and S speciation for the humic acid fraction of the Nordic Lake sample). The percentage of total S as reduced exocyclic S ranged from 23.6 to 46.9% (mean = 32.2±10.5%). We further assume that DOM S speciation is independent of total S content – recent data from Hoffmann *et al.*[7]and Poulin et al.[8] suggests, however, that the fraction of total S in reduced forms increases with increasing sulfurization. In that case, our application of a single conversion factor for total S to reduced S may underestimate the true contribution of DOM thiols to $Hg(II)_i$ binding. Other input parameters for modeling can be found in Table SI-3 below; for sulfide concentration, the mean of initial and final (t=3 h) concentrations were input into the speciation model. In modeling Hg-cysteine complexation, some reports suggest the possibility of a tris Hg(cys) complex (likely $Hg(Hcys)_3^-$.[9] Unfortunately, no thermodynamic data are available for this purported complex. Kõszegi-Szalai and Paál[10] reported equilibrium constants for Hg-penicillamine complexes, including a $Hg(Hpen)_3^-$ complex with a log K of 75.3 at I = 0 M. Given their similar structures (differing only in the two CH_3—substituents at the 3-position for penicillamine), we can evaluate the potential contributions of a $Hg(Hcys)_3^-$ complex to $Hg(II)_i$ speciation using the log K for the $Hg(Hgpen)_3^-$ complex. Using this approach, we find that $Hg(Hcys)_3^-$ is not likely to be a significant species under our experimental conditions ($[^{201}THg]$, $[H_2S]_T$, $[cys]_T$, and pH), and we do not include this species in our modeling. A summary of important thermodynamic data for speciation modeling can be found in Table SI-3 below.

Table SI-3. Thermodynamic data for equilibrium speciation modeling. Equilibrium constants for Hg-Cl and Hg-OH complexes were taken directly from the MINEQL+ database.

Reaction	***log K***	***Reference***
Hg-sulfide Aqueous Speciation		
$Hg^{2+} + 2HS^- = Hg(SH)_2^0$	39.1	Drott *et al.*[2]
$Hg^{2+} + 2HS^- = HgS_2H^- + H^+$	32.5	Drott *et al.*[2]
$Hg^{2+} + 2HS^- = HgS_2^{2-} + 2H^+$	23.2	Drott *et al.*[2]
Metacinnabar Precipitation		
$Hg^{2+} + HS^- = HgS(s) + H^+$	36.8	Drott *et al.*[2]
Hg-DOM Complexation		
$Hg^{2+} + 2RS^- = Hg(SR)_2$	42.0	Skyllberg[4]
$RS^- + H^+ = RSH$	10.0	Skyllberg[4]
Hg-CYS Complexation		
$Hg^{2+} + 2H^+ + 2CYS^{2-} = Hg(HCYS)_2^0$	64.1	Starý and Kratzer.[11]
$Hg^{2+} + 2CYS^{2-} = Hg(CYS)_2^{2-}$	43.9	Starý and Kratzer.[11]

Table SI-4. Summary of experimental variables in Hg methylation assays with *Desulfovibrio desulfuricans* ND132 in the presences of sulfurized DOM samples. DOM isolates were sulfurized as described in the main text, resulting in the S/C ratios reported in the table below. Reported values are means and standard deviations (*n* =3, excepting NLFA experiments, where *n* =2). n.d. = not determined due to lost samples. Cell density is average cell density measured at beginning and end of 3h incubation which typically increased less than 5% over the duration of the experiment.

DOM Isolate or Control	[DOC] (mg/L)	Measured S/C ratio (mmol S/mol C)	Cell density (x 10^8 cells/mL)	pH	Initial sulfide (µM)	Final sulfide (µM)	Total ^{201}Hg in medium (nM)	Total filterable ^{201}Hg (nM)	Total $Me^{201}Hg$ in medium (pM)
SRHA	9.19	3.42	5.68±0.21	7.27±0.01	2.25±0.05	3.62±0.12	0.30±0.16	0.21±0.01	39.6±4.9
SRHA	9.52	4.12	5.57±0.22	7.31±0.01	2.67±0.26	3.92±0.02	0.30±0.05	0.29±0.04	66.4±1.3
SRHA	9.58	4.73	5.32±0.31	7.25±0.01	3.36±0.08	4.15±0.11	0.32±0.06	0.26±0.04	80.7±1.5
SRHA	9.59	6.12	5.67±0.19	7.20±0.01	4.18±0.24	4.40±0.06	0.31±0.01	0.23±0.004	95.8±1.2
SRHA	9.24	5.83	5.43±0.09	7.33±0.02	3.72±0.17	4.53±0.10	0.39±0.02	0.24±0.01	128.4±1.9
SRFA	10	1.88	4.55±0.82	7.28±0.04	2.33±0.10	3.01±0.29	0.057±0.003	0.028±0.004	24.0±0.6
SRFA	10	3.80	5.75±1.51	7.28±0.04	2.79±0.29	3.22±0.20	0.070±0.008	0.034±0.007	40.5±1.6
SRFA	10	4.22	5.15±0.38	7.29±0.02	2.88±0.10	3.36±0.06	0.083±0.007	0.054±0.014	52.5±2.9
SRFA	10	4.08	5.03±0.52	7.22±0.02	2.87±0.03	3.44±0.14	0.13±0.01	0.088±0.007	86.6±0.2
SRFA	10	5.69	4.74±0.26	7.26±0.02	3.58±0.25	3.76±0.20	0.26±0.001	0.12±0.02	160±8
NLFA	10	3.12	1.44±0.21	7.52±0.12	0.26±0.18	0.95±0.83	0.15±0.07	0.067±0.006	36.9±11.4
NLFA	10	3.98	1.50±0.15	7.74±0.05	0.10±0.04	0.33±0.06	0.099±0.003	0.086±0.006	53.4±13.6
NLFA	10	8.83	1.36±0.18	7.61±0.10	0.05±0.01	0.42±0.31	0.10±0.01	0.090±0.01	49.5±13.4
NLFA	10	12.8	1.66±0.07	7.66±0.04	0.30±0.06	0.42±0.11	0.15±0.01	0.17±0.01	138±9
PLFA	8.3	11.0	4.79±0.23	7.35±0.02	3.99±0.27	6.44±0.78	0.13±0.004	0.018±0.002	39.2±4.0
PLFA	8.3	10.4	5.11±0.45	7.35±0.05	5.13±0.52	6.87±0.47	0.13±0.003	0.036±0.006	64.2±6.3
PLFA	8.3	14.5	4.76±0.33	7.34±0.05	5.13±0.52	7.02±0.28	0.12±0.01	0.038±0.002	53.0±7.0
PLFA	8.3	12.5	5.28±0.37	7.28±0.06	4.78±0.19	6.72±0.54	0.11±0.01	0.030±0.008	62.1±10.7
PLFA	8.3	12.2	5.80±0.89	7.32±0.02	5.13±0.52	6.56±0.26	0.11±0.01	0.049±0.008	57.8±0.8
500 µM L-cysteine control (SRHA)	N/A	N/A	5.74±0.13	7.28±0.00	5.78±0.11	19.3±0.1	0.46±0.02	0.07±0.01	362±6
500 µM L-cysteine control (SRFA)	N/A	N/A	4.04±0.67	7.14±0.00	5.55±0.72	31.1±4.9	0.37±0.02	0.28±0.02	308±11
500 µM L-cysteine control (NLFA)	N/A	N/A	1.43±0.17	7.30±0.06	0.28±0.10	4.08±3.1	0.13±0.02	n.d.	43.4±13.4
500 µM L-cysteine control (PLFA)	N/A	N/A	5.15±0.45	7.23±0.04	5.90±0.88	17.0±0.7	0.31±0.07	0.39±0.01	347±20
No DOM control (SRHA)	N/A	N/A	5.31±0.34	7.40±0.01	3.64±0.13	2.75±0.1	0.28±0.02	0.25±0.01	2.2±0.2
No DOM control (SRFA)	N/A	N/A	3.81±0.10	7.20±0.12	2.74±0.25	3.22±0.53	0.064±0.007	0.007±0.005	6.5±1.2

Table SI-5. Predicted equilibrium speciation of inorganic Hg(II) based on measured total ^{201}Hg in medium, pH, sulfide, DOC, and S/C ratio of DOM. $Hg(SR)_2$ is a two-coordinate complex of $Hg(II)_i$ with organic thiols; $Hg(SH)_2$ is the equivalent complex with inorganic sulfide.

DOM Isolate or Control	$[RSH]_T$ (μM)	[Meta-cinnabar] (M)	$[Hg(SR)_2]$ (M)	$[Hg(SH)_2]$ (M)	$[HgS_2H^-] + [HgS_2^{2-}]$ (M)	Total dissolved Hg (M)
SRHA	0.62	1.77×10^{-10}	7.28×10^{-15}	1.65×10^{-11}	1.06×10^{-10}	1.23×10^{-10}
SRHA	0.77	1.60×10^{-10}	1.08×10^{-14}	1.74×10^{-11}	1.23×10^{-10}	1.40×10^{-10}
SRHA	0.89	1.65×10^{-10}	1.15×10^{-14}	2.18×10^{-11}	1.33×10^{-10}	1.55×10^{-10}
SRHA	1.15	1.36×10^{-10}	1.55×10^{-14}	2.69×10^{-11}	1.47×10^{-10}	1.74×10^{-10}
SRHA	1.06	2.14×10^{-10}	1.69×10^{-14}	2.10×10^{-11}	1.55×10^{-10}	1.76×10^{-10}
SRFA	0.40	undersaturated	1.70×10^{-15}	7.50×10^{-12}	4.94×10^{-11}	5.69×10^{-11}
SRFA	0.80	undersaturated	6.44×10^{-15}	9.24×10^{-12}	6.09×10^{-11}	7.01×10^{-11}
SRFA	0.88	undersaturated	9.12×10^{-15}	1.07×10^{-11}	7.18×10^{-11}	8.25×10^{-11}
SRFA	0.85	undersaturated	1.19×10^{-14}	1.90×10^{-11}	1.09×10^{-10}	1.28×10^{-10}
SRFA	1.19	1.02×10^{-10}	2.13×10^{-14}	2.10×10^{-11}	1.32×10^{-10}	1.53×10^{-10}
NLFA	0.84	1.21×10^{-10}	1.00×10^{-13}	2.18×10^{-12}	2.54×10^{-11}	2.77×10^{-11}
NLFA	1.06	8.73×10^{-11}	6.80×10^{-13}	5.20×10^{-13}	1.03×10^{-11}	1.15×10^{-11}
NLFA	2.36	9.30×10^{-11}	3.00×10^{-12}	5.81×10^{-13}	8.42×10^{-12}	1.20×10^{-11}
NLFA	3.42	1.32×10^{-10}	3.77×10^{-12}	9.70×10^{-13}	1.59×10^{-11}	2.06×10^{-11}
PLFA	3.55	undersaturated	9.18×10^{-14}	1.53×10^{-11}	1.19×10^{-10}	1.34×10^{-10}
PLFA	3.39	undersaturated	6.34×10^{-14}	1.53×10^{-11}	1.19×10^{-10}	1.35×10^{-10}
PLFA	4.70	undersaturated	1.08×10^{-13}	1.44×10^{-11}	1.09×10^{-10}	1.24×10^{-10}
PLFA	5.75	undersaturated	7.14×10^{-14}	1.38×10^{-11}	9.11×10^{-11}	1.05×10^{-10}
PLFA	5.85	undersaturated	7.21×10^{-14}	1.35×10^{-11}	9.74×10^{-11}	1.11×10^{-10}
500 μM L-cysteine control (SRHA)	500	undersaturated	4.60×10^{-10}	2.43×10^{-19}	1.68×10^{-14}	4.60×10^{-10}
500 μM L-cysteine control (SRFA)	500	undersaturated	1.27×10^{-10}	7.12×10^{-17}	9.94×10^{-15}	1.27×10^{-10}
500 μM L-cysteine control (NLFA)	500	undersaturated	3.09×10^{-10}	6.09×10^{-17}	3.56×10^{-16}	3.09×10^{-10}
500 μM L-cysteine control (PLFA)	500	undersaturated	3.71×10^{-10}	2.59×10^{-15}	1.23×10^{-14}	3.71×10^{-10}
No DOM control (SRHA)	0	1.33×10^{-10}	0	1.44×10^{-11}	1.26×10^{-10}	1.40×10^{-10}
No DOM control (SRFA)	0	undersaturated	0	9.91×10^{-12}	5.41×10^{-11}	6.40×10^{-11}

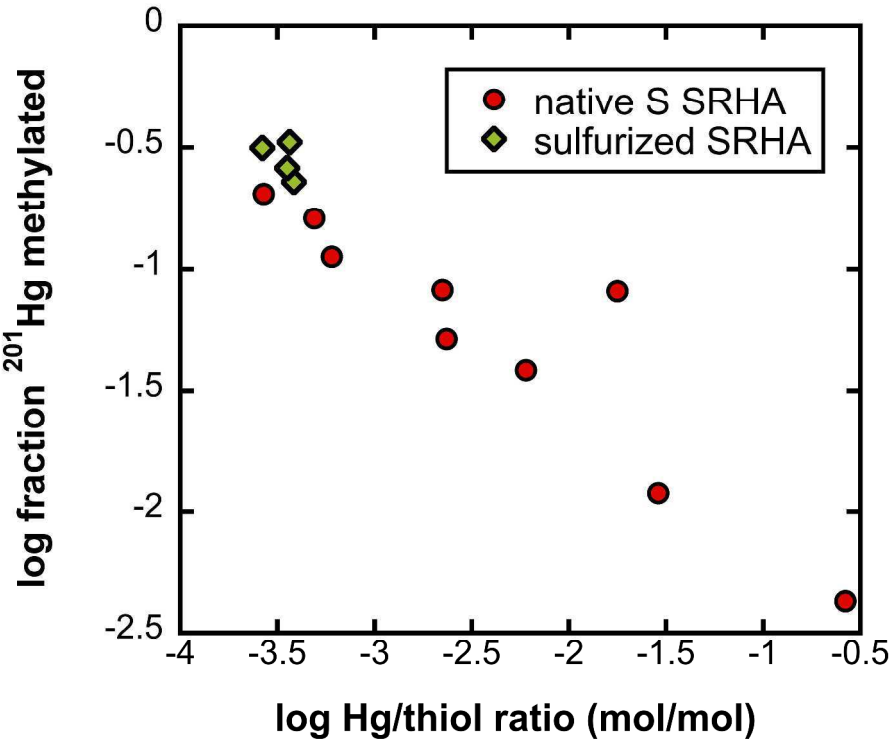

Figure SI-1. Relationship between log Hg/thiol ratio and log fraction ^{201}Hg methylated in solutions containing Suwannee River humic acid (SRHA), sulfide, and $^{201}HgCl_2$. Data for native SRHA include data from this study and from Graham et al.[12] Data for sulfurized SRHA from this study only. Thiol concentrations were estimated based on measured S/C ratio for SRHA samples and the assumption that 70% of total DOM S was thiols.

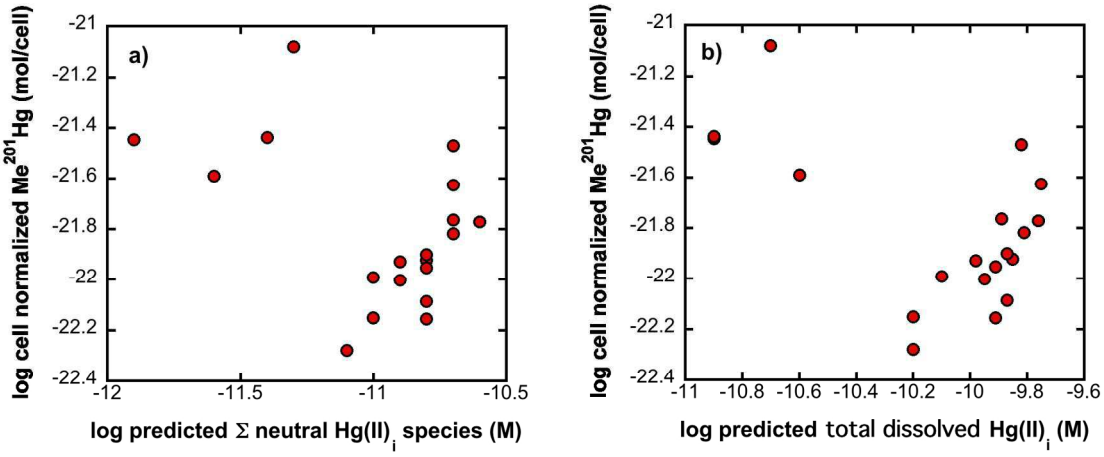

Figure SI-2. Correlations between the sum of neutral $Hg(II)_i$ species (**panel a**) or total dissolved $Hg(II)_i$ (**panel b**) and cell-normalized MeHg production. MeHg production cell-normalized due to significant differences in cell density between experiments. Data log-transformed due to non-normal distributions.

References for Supporting Information

1. Helms, J. R. *et al.* Absorption spectral slopes and slope ratios as indicators of molecular weight, source, and photobleaching of chromophoric dissolved organic matter. *Limnol Oceanogr* **53,** 955–969 (2008).
2. Drott, A., Björn, E., Bouchet, S. & Skyllberg, U. Refining thermodynamic constants for mercury(II)-sulfides in equilibrium with metacinnabar at sub-micromolar aqueous sulfide concentrations. *Environ Sci Technol* **47,** 4197–4203 (2013).
3. National Institute of Standards and Technology. NIST Critically Selected Stability Constants of Metal Complexes.
4. Skyllberg, U. Competition among thiols and inorganic sulfides and polysulfides for Hg and MeHg in wetland soils and sediments under suboxic conditions: Illumination of controversies and implications for MeHg net production. *J Geophys Res-Biogeo* **113,** G00C03 (2008).
5. Haitzer, M., Aiken, G. & Ryan, J. Binding of mercury(II) to dissolved organic matter: The role of the mercury-to-DOM concentration ratio. *Environ Sci Technol* **36,** 3564–3570 (2002).
6. Manceau, A. & Nagy, K. L. Quantitative analysis of sulfur functional groups in natural organic matter by XANES spectroscopy. *Geochim Cosmochim Acta* **99,** 206–223 (2012).
7. Hoffmann, M., Mikutta, C. & Kretzschmar, R. Bisulfide reaction with natural organic matter enhances arsenite sorption: Insights from X-ray absorption spectroscopy. *Environ Sci Technol* **46,** 11788–11797 (2012).
8. Poulin, B. A. *et al.* Spatial dependence of reduced sulfur in Everglades dissolved organic matter controlled by sulfate enrichment. *Environ Sci Technol* **51**, 3630-3639 (2017).
9. Schaefer, J. K. & Morel, F. M. M. High methylation rates of mercury bound to cysteine by Geobacter sulfurreducens. *Nature Geoscience* **2,** 123–126 (2009).
10. Koszegi-Szalai, H. & Paal, T. L. Equilibrium studies of mercury (II) complexes with penicillamine. *Talanta* **48,** 393–402 (1999).
11. Stary, J. & Kratzer, K. Radiometric determination of stability-constants of mercury species complexes with L-cysteine. *J Radioan Nucl Ch Le* **126,** 69–75 (1988).
12. Graham, A. M., Aiken, G. R. & Gilmour, C. C. Dissolved organic matter enhances microbial mercury methylation under sulfidic conditions. *Environ Sci Technol* **46,** 2715–2723 (2012).